Sepsis Induces Age- and Sex-Specific Chromatin Remodeling in Myeloid-Derived Suppressor Cells

Angel M. Charles,[1] Christine E. Rodhouse,[1] Dijoia B. Darden,[1] Marie-Pierre L. Gauthier,[2] Mingqi Zhou,[2,8] Miguel Hernandez-Rios,[1] Dayuan Wang, [1,3] Gemma Casadesus,[4] Letitia Bible,[1] Alicia M. Mohr,[1] Feifei Xiao,[1] Guoshuai Cai,[1] Jason O. Brant,[3] Shannon M. Wallet,[5] Clayton E. Mathews,[6] Lyle L. Moldawer,[1] Paramita Chakrabarty,[7] Rhonda L. Bacher,[3] Philip A. Efron,[1] Robert Maile,[1] and Michael P. Kladde[1,2,5,*]

Affiliations:

[1]Sepsis and Critical Illness Research Center, Department of Surgery, College of Medicine, University of Florida, Gainesville, Florida, United States.

[2]Department of Biochemistry and Molecular Biology, College of Medicine, University of Florida, Gainesville, Florida, United States.

[3]Department of Biostatistics, College of Public Health & Health Professions, University of Florida, Gainesville, Florida, United States

[4]Department of Pharmacy and Therapeutics, University of Florida College of Medicine, Gainesville, FL, USA

[5]Department of Oral Biology, College of Dentistry, University of Florida, Gainesville, Florida, United States

[6]Department of Pathology, Immunology and Laboratory Medicine, College of Medicine, University of Florida, Gainesville, Florida, USA

[7]Department of Neuroscience, University of Florida College of Medicine, Gainesville, Florida, USA

[8]Present address: Jinhua Academy, Zhejiang Chinese Medical University, Jinhua, Zhejiang Province, 321032, China

*Correspondence:
Michael P. Kladde, Ph.D.
2033 Mowry Rd.
Box 103633
Gainesville, FL 32610-3633
ORCID: 0000-0001-7951-9291

Phone: (352) 273-8142
Email: kladde@ufl.edu

Keywords: precision medicine, myeloid-derived suppressor cells, sepsis, aging, sex, epigenetics

Word count: 6664

Figure and Table Count: 7 Figures, 1 Table, 3 Supplemental Figures and one Supplemental Table

SUMMARY

Sepsis survivors frequently develop long-term immune dysfunction, but the epigenetic mechanisms underlying persistent myeloid suppression remain unclear. Myeloid-derived suppressor cells (MDSCs), whose function is shaped by host age and sex, are key contributors to post-sepsis immune dysregulation. Here, we present a high-resolution epigenetic map targeting gene promoters of MDSCs after sepsis using MAPit-FENGC, a single-molecule assay that simultaneously profiles DNA methylation and chromatin accessibility. In a clinically relevant murine model including young and older adult male and female mice, splenic MDSCs were isolated for MAPit-FENGC and single-cell RNA sequencing. Unsupervised clustering identified nine promoter classes reflecting chromatin dynamics: age- and sex-dependent sepsis-induced opening (Classes 1-4), persistent closure with varying levels of DNA methylation (Classes 5-7), and constitutive openness post-sepsis (Classes 8, 9). Transcriptomic profiling corroborated these promoter states, linking accessibility with gene expression. These findings establish how epigenetic reprogramming of MDSCs may shape age- and sex-specific immune trajectories in sepsis survivors.

55 **INTRODUCTION**

56 Sepsis, when the host has organ insufficiency/failure in response to infection[1] affects in excess of
57 1.7 million adults in the United States, and results in the death of more than 350,000 of these
58 individuals.[2] In addition, sepsis is estimated to cost greater than $38 billion per year in America
59 alone.[3] Although acute hospital mortality has improved due to measures such as the Surviving
60 Sepsis campaign,[4] long-term patient outcomes remain dismal.[5,6] Despite the significance and
61 impact of all the former, few to no therapeutics are available for this patient population.[7]

62

63 Myeloid-derived suppressor cells (MDSCs), delineated almost two decades ago,[8] are defined as
64 pathologically activated myeloid cells with potent immunosuppressive activity, yet they also
65 possess some pro-inflammatory properties.[9] Although the leukocytes have been investigated in the
66 cancer field for some time, research focused on MDSCs in sepsis is relatively recent.[10] MDSCs
67 have been demonstrated to expand in number, remain circulating in the sepsis survivor, and are
68 associated with poor outcomes in these patients.[11,12] Whereas these sepsis-derived MDSCs meet
69 the key functional definition of MDSCs (immunosuppressive activity against lymphocytes, etc.),
70 data indicate that MDSCs from septic mice are not identical to oncologic-derived MDSCs, in both
71 mice and humans.[13-15] Modification of MDSCs in the sepsis survivor represents a potential
72 approach to improve these patients' outcomes,[16] but still requires a better disease-specific
73 understanding of these cells.

74

75 In addition to the need for more disease-specific precision/personalized therapeutics for sepsis,
76 there is a need to delineate how sepsis engenders unique effects in certain cohorts, e.g., age and
77 sex.[16-25] Work from our group and others has illustrated that both sex and age have significant

effects on the sepsis response, as well as on the post-infection MDSCs generated by that host.[17,18,20-22] Thus, investigating these cohorts will be key to any successful future interventions for sepsis survivors.

Epigenetics, the study of alterations in gene expression not due to changes in the genetic code, are considered a potential method of successfully modifying MDSCs in the host so that these cells will no longer be pathologic.[26] One such method of studying the epigenetics of the sepsis-induced MDSC is Methyltransferase Accessibility Protocol for Individual Templates combined with Flap-Enabled Next-Generation Capture (MAPit-FENGC), a validated method that allows for simultaneous single-molecular-level analysis of endogenous CpG methylation and accessibility at targeted promoter and enhancer regions.[27] Using a preclinical surgical sepsis animal model that better parallels the human condition,[17,21] we utilized MAPit to assess the epigenetic uniqueness of isolated murine splenic $Cd11b^{+}Gr1^{+}$ MDSCs across several cohorts: sepsis versus control, male versus female, and young adult versus older adult.

RESULTS

Sepsis exerted a profound and consistent remodeling of the MDSC epigenome. Promoters that regulate inflammatory, metabolic, and differentiation-associated programs displayed striking shifts in both accessibility and methylation patterns. Specifically, multiple gene promoters showed increased accessibility paired with reduced methylation, a configuration associated with transcriptional activation, while other loci demonstrated persistent closure and hypermethylation, consistent with durable repression. This dichotomy defined nine distinct promoter classes, of which Classes 1-4 reflected sepsis-induced opening, whereas Classes 5-7 and Classes 8, 9 captured

101 states with persistently closed (likely repressed) and constitutively open (likely expressed)
102 chromatin, respectively. Importantly, these global patterns were evident regardless of host age or
103 sex, underscoring sepsis itself as the primary driver of epigenetic reprogramming.
104

105 **Global epigenetic structure separates MDSCs by sepsis, age, and sex**

106 Principal Component Analysis (PCA) of MAPit-FENGC single-molecule data revealed clear
107 global distinctions (out to four PCs) in the epigenetic landscape of $CD11b^{+}Gr1^{+}$ splenic MDSCs
108 based on sepsis exposure, age, and sex (**Figures S1, S2**). In PCA of endogenous CpG methylation
109 alone (**Figure S1**), septic mice formed distinct clusters compared to naïve controls. Notably, older
110 adult females demonstrated the greatest divergence in CpG methylation patterns after sepsis,
111 suggesting age- and sex-dependent remodeling of the methylome. When PCA was restricted to
112 GpC methylation (chromatin accessibility) data (**Figure S2**), sepsis again drove marked
113 separation, particularly among female samples. Septic females (both young and older adult)
114 clustered distinctly from their naïve counterparts, whereas MDSCs derived from all adult males
115 displayed a more intermediate shift. This suggests that chromatin accessibility is broadly altered
116 by sepsis, with a stronger response in females.
117

118 **Distinct promoter accessibility classes exist in MDSCs following sepsis**

119 Unsupervised clustering analysis[28] of individual MAPit-FENGC promoter copies revealed nine
120 promoter classes (Classes 1-9) in splenic $CD11b^{+}Gr1^{+}$ MDSCs, each with characteristic chromatin
121 accessibility and DNA methylation patterns across conditions (**Table S1**). These classes captured
122 the range of epigenetic responses to sepsis and underline strong age- and sex-specific differences
123 in MDSC promoter regulation. Here, we describe qualitative trends for each class, highlighting

124 how sepsis-induced chromatin accessibility (nucleosome-free regions, NFRs) and DNA
125 methylation changes vary by promoter class, age, and sex.
126
127 ***1. Sepsis induces NFRs at many promoters (Classes 1-4)***
128 Several promoter classes exhibited marked chromatin opening due to nucleosome sliding/eviction
129 in response to sepsis. A single Class 1 promoter, *S100a9* (encoding the calcium-binding protein
130 A9, a key MDSC protein that regulates MDSC trafficking, expansion, and activation, as well as
131 acting as an alarmin),[29,30] showed dramatic, sepsis-driven increases in accessibility (at GCH sites;
132 each mouse, right within each pair of panels; yellow color; **Figure 1A**). Large NFRs, with peak
133 accessibility upstream of the transcription start site (TSS), formed on *S100a9* promoter copies in
134 five of six total septic female (**Figure 1A**) and male (not shown) mice. These NFRs were
135 characterized by promoter copies with continuous spans of accessible GCH of variable length—
136 some extending across the entire 523 bp assayed region. The magnitude of *S100a9* NFR formation
137 in Class 1 was modulated by sex and age. In MDSCs isolated from females, older septic mice had
138 significantly more extensive *S100a9* promoter opening than young septic females, whereas male
139 MDSCs showed robust *S100a9* NFR formation in sepsis regardless of age (though slightly less
140 pronounced than in females). In septic mice, *S100a9* demonstrated increased average chromatin
141 accessibility in older adult females compared to young adult females and older adult males, with
142 older females showing the largest NFRs and greatest fraction of molecules with NFRs (indicating
143 a higher proportion of cells with an open promoter; **Figure 1B**). This was accompanied by a
144 modest decrease in average CpG (at HCGs) methylation across the locus, most notably in the
145 proximal promoter region. This Class 1 promoter had moderate DNA methylation at baseline that

146 underwent partial demethylation upon sepsis, in line with an activated chromatin state (**Figure**
147 **1C**).
148
149 Class 2 promoters also gained accessibility in septic conditions but in a more context-dependent
150 manner. Specifically, Class 2 chromatin opened (NFRs appeared) in older adult female sepsis and
151 in male sepsis (both young and older), but not in young female sepsis. This pattern indicates that
152 young females failed to open these promoters unless aged, whereas males of either age mounted
153 an increase in accessibility. When present, the degree of NFR formation for Class 2 genes was
154 similar between sexes. A representative Class 2 gene is *Cxcr2* (**Figure 1D**; encodes C-X-C
155 chemokine receptor type 2, trafficking and facilitating the suppressive function of MDSCs within
156 inflamed tissue).[31] In MDSCs from septic hosts, the *Cxcr2* promoter remained nucleosome-
157 occupied (by randomly positioned nucleosomes) in young females but showed clear NFR
158 formation at the TSS in older females (and in males of both ages). Concordantly, *Cxcr2* and other
159 Class 2 promoters (e.g., *Nos2*, *Ptgs2*) exhibited low-to-moderate DNA methylation (at HCGs; left;
160 red color) that either remained stable or slightly decreased with sepsis in the responsive groups
161 (**Figure 1D**). The requirement of advanced age for female MDSCs to demonstrate open Class 2
162 loci, *versus* no such requirement in males, highlights a female-specific age dependency in
163 epigenetic activation of this promoter set. Average chromatin accessibility at the *Cxcr2* locus was
164 significantly increased in septic older adult mice, particularly females, consistent with an
165 epigenetic state favoring enhanced expression (**Figure 1E**). This accessibility gain was not
166 accompanied by substantial changes in DNA methylation (**Figure 1F**), which remained uniformly
167 low upstream of the TSS across groups, suggesting a permissive chromatin environment at
168 baseline, with further inducibility following septic challenge.

169

170 Class 3 promoters were broadly responsive to sepsis across all cohorts, with no significant sex or
171 age differences in their accessibility changes. These loci, e.g., *S100a8* (S100A8 acts similarly to
172 S100A9[29]) and *Mmp8* (MMP8 facilitates MDSC mobilization and migration, as well as the
173 immunosuppressive environment),[32] formed NFRs in MDSCs from septic hosts in both males and
174 females, and in both young and older mice, to a similar extent. As a result, Class 3 represents a
175 core set of promoters that are consistently opened by sepsis irrespective of host age or sex. DNA
176 methylation of Class 3 promoters was generally low to intermediate and showed modest changes
177 (often slight demethylation), if any, upon sepsis. The uniform NFR formation at these sites
178 suggests they may drive fundamental sepsis-responsive genes in MDSCs that are required in all
179 populations. For instance, *S100a8* (encodes the S100 calcium-binding protein A8) promoter
180 exhibited equivalent accessibility gains in septic males and females, young and older (data not
181 shown), mirroring the behavior of its Class 1 counterpart *S100a9*, but without the female-older
182 bias. Similarly, *Mmp8* (encoding matrix metalloproteinase-8) opened consistently in all septic
183 groups, forming an NFR over the TSS (**Figure 2A**). Thus, Class 3 promoters highlight sepsis-
184 induced epigenetic changes that are common to both sexes and ages, representing an invariant
185 component of the MDSC response to sepsis. *Mmp8* showed a sepsis-induced increase in chromatin
186 accessibility (**Figure 2B**) alongside a pronounced decrease in DNA methylation in its promoter
187 region (**Figure 2C**). These coordinated epigenetic modifications suggest enhanced transcriptional
188 readiness.

189

190 In contrast, a single Class 4 promoter displayed a clear sex-specific accessibility pattern. This
191 promoter, *Fyb*, drives expression of adhesion and degranulation adaptor protein (ADAP), a

192 signaling adaptive protein hypothesized to support MDSC migration, suppressive activity, and
193 survival.[33] *Fyb* promoter demonstrated TSS-localized NFRs in older and young adult naïve mice
194 (**Figure 2D**), and an increased number of NFR-containing MDSCs from septic female mice of
195 both ages. Concomitantly, in septic mice, an upstream region of accessibility in naïve mice became
196 inaccessible in a subset of *Fyb* promoter molecules after septic shock (**Figure 2D;** green rectangle).
197 In contrast, septic males (older or young) showed no detectable increase in chromatin opening or
198 the concomitant protection beyond the initial accessibility of the *Fyb* TSS region in naïve male
199 mice of both ages. The average chromatin accessibility plot reveals increased and decreased
200 accessibility in MDSCs from septic mice compared to naïve controls over the TSS region and
201 upstream regulatory elements of *Fyb*, respectively (**Figure 2E**). Complementary to this, the
202 average methylation track shows DNA methylation levels at the Class 4 *Fyb* promoter were rather
203 low at baseline and showed further demethylation in female sepsis, especially in older mice,
204 consistent with an epigenetic landscape that supports transcriptional activation in females (**Figure**
205 **2F**). The absence of any chromatin change in males, despite an adequate sepsis insult (as verified
206 by other classes), emphasizes a sex divergence in epigenetic regulation, with preferential activation
207 of the Class 4 locus in MDSCs from female mice during sepsis.
208
209 ***2. Persistently closed promoters remain refractory to induction in sepsis (Classes 5-7)***
210 In contrast to the sepsis-inducible classes above, chromatin at Class 5-7 loci was closed with no
211 formation of an NFR in any group (naïve or septic, male or female, young or older). Instead,
212 accessibility was limited to relatively short linkers distributed across each promoter, indicating
213 that their DNA was packaged into arrays of randomly positioned nucleosomes. Notably, linker
214 accessibility in Class 5-7 promoters decreased in MDSCs isolated from septic mice (older females

215 and males) and young septic male mice. Therefore, Classes 5-7 represent promoters that underwent
216 sepsis-specific loss of linker accessibility in an age- and sex-driven manner, contrasting with the
217 NFR formation observed in Class 1-4 promoters.
218
219 The distinction between Classes 5, 6, and 7 lies in their DNA methylation status: Class 5 promoters
220 were generally characterized by high levels of endogenous DNA methylation at all CpGs
221 (hypermethylation), which is consistent with a silenced state; Class 6 promoters exhibited
222 moderate-to-high CpG methylation (typically showing little to no demethylation); and Class 7
223 promoters had low baseline methylation. Despite these differences, all three classes demonstrated
224 a sepsis-specific loss of accessibility in older mice (male and female), and to a lesser extent, in
225 young adult male mice.
226
227 Representative Class 5 genes include *Lyz1* (lysozyme 1), *Retn* (resistin), and *F7* (coagulation factor
228 VII), among others (**Figure 3A-C**). After sepsis, these promoters exhibited minimal change in
229 DNA methylation but showed decreased linker accessibility, specifically, in older adult mice (both
230 sexes) and in young males. For example, *Lyz1* promoter remained highly methylated, with no
231 visible formation of large NFRs capable of supporting active transcription in MDSCs from either
232 naive or septic mice. Similarly, *Retn* showed no NFR formation in any condition, although its
233 methylation level declined slightly in older sepsis compared to older naïve animals.
234
235 Exemplifying Class 6, the *Serpine1* promoter, encoding the fibrinolytic serine protease inhibitor
236 Pai-1, a protein that influences the presence and activity of MDSCs, often promoting
237 immunosuppression and tumor growth)[34] was occupied by arrays of randomly positioned

238 nucleosomes in naïve control mice (**Figure 3D-F**). Similar to Class 5 promoters, much of this
239 characteristic linker accessibility was diminished in MDSCs from older septic mice (**Figure 3D**).
240 Average chromatin accessibility plots show that *Serpine1* is less accessible in septic groups,
241 particularly in older mice, and to a lesser extent, young males, compared to their naïve counterparts
242 (**Figure 3E**). No true DNA demethylation was detected (**Figure 3F**; the apparent demethylation
243 of five CpG sites around map position 423 bp in MDSCs from some septic mice is due to off-
244 target methylation by M.CviPI at accessible CCG sites (region highlighted red), and therefore
245 instead reflects loss of chromatin accessibility at those CCGs). Despite baseline CpG methylation
246 at the Serpine 1 TSS (map position 367 bp), the chromatin state of the *Serpine1* promoter is
247 consistent with strong transcriptional silencing due to occupancy by randomly positioned
248 nucleosomes and absence of NFRs. Given the role of *Serpine1* in inflammation, tissue remodeling,
249 and coagulopathy, this decreased accessibility may reflect impaired inflammatory reprogramming
250 of MDSCs during sepsis.
251
252 A Class 7 example is the *Vcan* gene (**Figure 3G-I**) that encodes Versican, an extracellular matrix
253 component that is upregulated during sepsis and thought so have some immune regulatory
254 properties.[35,36] Similar to Class 5 and 6 genes, the *Vcan* promoter in MDSCs from young or naïve
255 female mice had no large NFRs, only displaying linker accessibility in arrays of randomly
256 positioned nucleosomes (**Figure 3G**). However, as was observed for Class 5 and 6 loci, in MDSCs
257 from older septic females, this characteristic linker accessibility diminished. Average chromatin
258 accessibility across the *Vcan* promoter revealed a modest but consistent decrease in septic
259 conditions, particularly in older, but not young, adult female mice (**Figure 3H**). Male adult septic
260 mice (young and older) showed reduced average accessibility across the *Vcan* promoter, although

261 the effect was less pronounced than that observed in older adult septic females. Conversely, young
262 female and naïve adult male mice showed relatively higher accessibility, suggesting age- and sex-
263 specific regulation. Again, no true DNA demethylation was observed at this locus and all
264 subsequent loci; instead, only decreased accessibility at CCG sites was detected (**Figure 3I**).
265

266 ***3. Promoters with constitutive NFRs that largely remain refractory to sepsis (Class 8)***

267 Class 8 gene promoters showed high accessibility, with prominent NFRs encompassing the TSSs
268 in all four conditions. However, these promoters illustrated an age-dependent, relatively modest
269 loss of NFR accessibility in MDSCs from only older septic female mice, where overall NFR
270 architecture and presumably transcriptional activity was largely preserved. Class 8 promoters
271 generally exhibited low, baseline DNA methylation levels, reflective of their active status.
272

273 An example of Class 8 is the *Cd274* gene (**Figure 4A-C**), encoding the immune-checkpoint
274 inhibitor PD-L1, which in MDSCs plays a direct role in suppressing T-cell responses.[38] The *Cd274*
275 promoter exhibited the highest levels of NFR accessibility in MDSCs from young septic mice and
276 in naïve adult controls. MDSCs from older adult septic females showed a modest reduction in NFR
277 accessibility but retained NFR structure, consistent with ongoing transcriptional activity. Average
278 accessibility at the *Cd274* locus was modestly decreased in MDSCs from older adult septic female
279 mice compared to naïve controls and young septic mice (**Figure 4B**). MDSCs from septic animals,
280 particularly older individuals, showed a modest decrease in accessibility. Excluding DNA
281 methylation of accessible CCG sites, only basal CpG methylation levels were detected within
282 *Cd274* regulatory sequences, consistent with permissive chromatin and potential gene expression
283 (**Figure 4C**).

284

285 Other Class 8 genes, such as *Nfkbiz* (encoding the NF-κB inhibitor IκBζ; **Figure 4D-F**), *Vdr*
286 (vitamin D receptor), *Il4ra* (IL-4 receptor α chain, which has been shown to be important to
287 MDSC-suppressive activity),[39] and *Atf6* (ATF6, a transcription factor that activates target genes
288 for the unfolded protein response) all followed a similar pattern with NFRs present in all conditions
289 except in MDSCs from older septic female mice. In each case, MDSCs from the older female
290 septic group showed baseline CpG methylation (omitting CCG) and a modest loss of promoter
291 accessibility that is unlikely to impair transcriptional activity.

292

293 ***4. Constitutively accessible promoters that maintain open chromatin in all conditions (Class 9)***
294 Finally, a small subset of promoters (Class 9) remained highly accessible across all conditions,
295 largely unaffected by sepsis, age, or sex. Class 9 promoters had pre-existing, prominent
296 nucleosome-free regions in naïve MDSCs and retained these open states after the stress of sepsis.
297 They also displayed low basal DNA methylation, consistent with active promoters. A clear
298 example is the *Tet2* promoter, which encodes the DNA demethylation enzyme Tet2 (**Figure 5**).
299 The *Tet2* promoter showed prominent NFRs in all samples across all conditions indicating
300 constitutive chromatin accessibility. CpG methylation could not be assessed because out of 35
301 HGCs in the *Tet2* promoter amplicon all are CCGs.

302

303 ***Single-cell transcriptomics support epigenetic promoter class distinctions in MDSC subsets***
304 To determine whether promoter accessibility classes defined by MAPit-FENGC corresponded to
305 functional gene expression patterns, we analyzed single-cell RNA-seq data from $CD11b^{+}Gr1^{+}$
306 splenic leukocytes isolated from young and older, male and female adult mice under naïve or septic

307 conditions, collected in the Companion Paper (Rodhouse et al.). Data were stratified into three
308 MDSC subtypes: early MDSCs (E-MDSC), monocytic MDSCs (M-MDSC), and granulocytic
309 MDSCs (PMN-MDSC) based on gene expression patterns. The gene *S100a9*, assigned as a Class
310 1 promoter and characterized by widespread NFR formation in all septic groups, was induced
311 across all three MDSC subsets in response to sepsis, regardless of age or sex (**Figure 6**). This
312 transcriptional profile matches the broadly accessible chromatin configuration observed
313 epigenetically. Similarly, the Class 3 promoter *S100a8*, which formed sepsis-induced NFRs in
314 young and older mice, displayed upregulation in E-MDSCs and PMN-MDSCs during sepsis. In
315 contrast, a Class 6 promoter *Ccl5*, which remained epigenetically inaccessible in all conditions,
316 showed only modest and selective transcriptional induction in a subset of MDSCs, primarily E-
317 and M-MDSCs, in young male septic mice (**Figure 7)**. These observations are consistent with a
318 transcriptionally repressed or enhancer-driven regulatory program.
319
320 In contrast, *Nfkbiz*, assigned to Class 8 based on selective modest promoter closure in "Aged
321 Sepsis," showed relatively low but detectable expression across MDSC subsets. While MAPit-
322 FENGC revealed loss of promoter accessibility specifically in aged sepsis mice, scRNA-seq
323 analysis did not show consistent transcriptional silencing in this group. Instead, modest expression
324 changes were observed in PMN-MDSCs and E-MDSCs, particularly in young female septic mice.
325 *Tet2*, a representative Class 9 gene whose promoter remained consistently accessible across all
326 MAPit-FENGC conditions, exhibited modest transcriptional activation in scRNA-seq, primarily
327 during sepsis in M-MDSCs. Despite the stable chromatin accessibility across all groups,
328 expression was low or unchanged in E-MDSCs and PMN-MDSCs.
329

330 **DISCUSSION**

331 Our study provides a high-resolution, single-molecule epigenetic map of splenic MDSCs in a
332 murine model of surgical sepsis, revealing how host age and sex shape chromatin accessibility and
333 DNA methylation in this immunoregulatory cell type. Using MAPit-FENGC, we identified nine
334 distinct promoter classes across multiple immune-relevant loci, encompassing a spectrum of
335 response classes ranging from sepsis-induced chromatin opening to age-specific silencing. These
336 epigenetic patterns were tightly linked to host sex, age, and sepsis exposure and corresponded to
337 changes in transcription, as assessed by scRNA-seq.

338

339 We discovered an age-dependent epigenetic repression of key immunoregulatory genes (e.g.,
340 *Cd274*, *Nfkbiz*, *Il4ra*) in older septic mice (Class 8). These promoters exhibited basal CpG
341 methylation and robust promoter NFR accessibility in young or naïve mice. Older septic females
342 showed a modest loss of accessibility but retention of NFR structure, consistent with ongoing
343 transcriptional activity. Therefore, nucleosome repositioning emerges as the dominant mechanism
344 of transcriptional repression in MDSCs from aged hosts. The selective, partial closure of immune
345 checkpoint and anti-inflammatory loci (e.g., *Cd274*, *Il10*) may impair key MDSC functions (T-
346 cell suppression and inflammation resolution), which rely on PD-L1 and IL-10 expression. In aged
347 septic hosts, epigenetic repression of these genes may render MDSCs less effective or
348 dysregulated, contributing to the persistent immune dysfunction and chronic critical illness seen
349 in this population.[16,21]

350

351 In contrast, sepsis-induced chromatin opening was observed in promoter classes associated with
352 canonical MDSC effector genes (Classes 1-4). Promoters such as *S100a9*, *S100a8*, *Nos2*, and

353 *Ptgs2* gained accessibility in septic MDSCs, often with concurrent demethylation, consistent with
354 transcriptional activation.[29,40] The magnitude of these chromatin changes varied by sex and age.
355 For example, Class 1 (*S100a9*) was accessible across all septic groups but showed particularly
356 robust NFR formation in older females. These findings suggest that both age and sex can influence
357 *S100a9* expression and chromatin accessibility, potentially contributing to the observed robust
358 NFR formation at the *S100a9* promoter in older females during sepsis. Research has demonstrated
359 that chromatin accessibility at the *S100a9* promoter is regulated during monocyte differentiation
360 and is influenced by transcription factors such as C/EBPδ. In particular, C/EBPδ has been shown
361 to bind within the *S100a9* promoter region, affecting its accessibility and expression levels.[41] Age-
362 related changes in immune function ("inflammaging") have been associated with alterations in
363 inflammatory markers, including S100a9. For example, a study investigating the impact of age
364 and sex on inflammatory markers found that aging is associated with higher expression of *S100a9*
365 and components of the NLRP3 inflammasome independent of sex[42]. In the context of systemic
366 lupus erythematosus (SLE), S100a9 has been identified as a molecule integral in determining sex-
367 specific immune responses,[30] which may be relevant to understanding its regulation in other
368 inflammatory conditions like sepsis. The *S100a8* and *S100a9* promoters (Class 1 and 3 in MAPit)
369 exhibit universal sepsis-induced opening, particularly in aged females, and these genes are also
370 among the top differentially expressed genes in our scRNA-seq dataset (in the accompanying
371 manuscript, Rodhouse et al.). This gene pair is pivotal in MDSC activation, trafficking, and
372 suppressive function. The robust accessibility and expression of *S100a8*/*a9* in both studies
373 supports their role as central, sepsis-responsive effectors and potential biomarkers of MDSC
374 reprogramming.
375

376 Class 2 promoters opened only in older females and males, but not young females highlighting a
377 female-specific age threshold for epigenetic activation at specific loci. For example, CXCR2 is a
378 chemokine receptor primarily expressed on neutrophils and plays a crucial role in mediating their
379 recruitment to sites of infection, essential for survival in sepsis. Excessive or dysregulated CXCR2
380 signaling can contribute to tissue damage and organ failure,[43] and the observed increased
381 accessibility of the CXCR2 gene in older females and males may suggest an age-related epigenetic
382 regulation leading to enhanced expression.
383
384 The identification of stably closed promoters (Class 5) and constitutively open loci (Class 9) may
385 further describe the epigenetic plasticity in MDSCs. Class 5 genes (e.g., *Lyz1*, *F7*) remained
386 silenced through hypermethylation and packaging into arrays of randomly positioned nucleosomes
387 regardless of condition. The refractoriness of Class 5 promoters to opening indicates they are
388 epigenetically "locked down" in splenic MDSCs. These genes remain transcriptionally inactive
389 even in sepsis, suggesting they are either irrelevant to the MDSC sepsis response or otherwise
390 tightly repressed in this cell type.
391
392 Classes 6 and 7 highlight additional promoters shut down in MDSCs. Although these promoters
393 had less DNA methylation than Class 5 promoters, they nevertheless remained epigenetically
394 repressed as gauged by inability to form large NFRs following CLP sepsis challenge. Like Class
395 5, the chromatin of Class 6 and 7 promoters consists of randomly positioned nucleosomes with
396 accessible linker DNA. Across Class 6 and 7 promoters, we frequently observed that all MDSC
397 samples from older septic mice lacked NFRs, whereas one or more of the other conditions retained
398 an accessible configuration, suggesting age-specific chromatin condensation at these promoters.

399 Across Class 6 and 7 promoters, all MDSC samples from older septic mice consistently lacked
400 NFRs characteristic of active promoters, while one or more of the other conditions retained
401 localized linker accessibility. This pattern indicates age-specific chromatin condensation within
402 promoter regions that are normally permissive, rather than a global loss of linker accessibility. As
403 with all Class 5-7 promoters, these loci remain devoid of canonical NFRs, distinguishing them
404 from the open promoter architectures observed in Classes 1-4.
405
406 Class 8 includes several immune-related genes (e.g., *Cd274*, *Il4ra*, *Nfkbiz*) whose partially
407 diminished accessibility in older survivors of sepsis might contribute to impaired or altered
408 immune regulation in this cohort. Notably, several Class 5–8 promoters, including *Cd274* (PD-
409 L1), *Il10*, and *Nfkbiz*, exhibited significant chromatin closure selectively in MDSCs from older
410 septic mice. This pattern suggests a dominant role for nucleosome occupancy in regulating gene
411 expression in aged hosts. Supporting this, our companion transcriptomic study (Rodhouse et al.)
412 demonstrated that these genes were only modestly or minimally induced at the RNA level in older
413 MDSC populations following sepsis, particularly in M-MDSCs. These findings support the
414 concept that age-associated epigenetic silencing of immunoregulatory loci may cause persistent
415 immune dysfunction in older sepsis survivors, and that transcriptional non-responsiveness may be
416 epigenetically preconditioned in this cohort.
417
418 Class 9 promoters (e.g., *Tet2*) were persistently accessible across all groups, suggesting these are
419 "core" MDSC housekeeping genes that remain transcriptionally poised or active even in the face
420 of sepsis-induced stress, are simply important for the development of this cell type (the
421 demethylation enzyme TET2 is highly expressed in hematopoietic stem and progenitor cells and

422 has been shown to be essential in regulating MDSC numbers in tumor models[44] and models of
423 emergency myelopoiesis post-LPS-challenge).[45] Generally, Class 9 genes appear to be core
424 functional genes whose promoter chromatin is stably open as part of the identity or necessary
425 function of MDSCs. Their invariant accessibility contrasts the dynamic changes seen in Classes 1-
426 8. The presence of Class 9 promoters underscores that some key promoters remain epigenetically
427 unaltered and continuously active throughout sepsis. Maintenance of a large NFR at the *Tet2*
428 promoter in all conditions exemplifies this stability. We did not observe any loss of accessibility
429 at Class 9 loci, reinforcing that these promoters are resilient to both inflammatory stress and host
430 factors.
431
432 These context-specific activation patterns suggest that MDSC-mediated immunosuppression may
433 arise *via* different regulatory programs in males versus females, and in young versus older hosts.
434 This observation aligns with our prior data on age- and sex-specific differences in MDSC
435 transcriptomes and function,[17,19] and may provide mechanistic insight into how such differences
436 are epigenetically encoded.
437
438 Importantly, single-cell transcriptomics supported many of the epigenetic patterns described.
439 Genes in Classes 1 and 3 showed increased expression in MDSC subsets concordant with sepsis-
440 induced chromatin opening. In contrast, Class 8 genes (e.g., *Nfkbiz*, *Il4ra*) showed partial
441 decoupling between accessibility and expression in older septic MDSC raising the possibility of
442 additional regulatory checkpoints, such as enhancer silencing or post-transcriptional control,
443 particularly in aged immune cells.[13,26] These findings underscore the importance of integrating
444 multiple levels of gene regulation (chromatin state, methylation, and transcription) when

445 evaluating MDSC behavior in critical illness. Collectively, these scRNA-seq results support the
446 biological relevance of the MAPit-defined promoter classes, illustrating how chromatin
447 accessibility states correspond to transcriptional outcomes across sepsis, sex, and age in MDSC
448 subsets.
449
450 The epigenetic heterogeneity observed here helps explain the divergent immune
451 phenotypes/endotypes that we[46,47] have defined in sepsis survivors, and provides a foundation for
452 understanding MDSC dysfunction in aging. In particular, the age-specific silencing of checkpoint
453 and anti-inflammatory loci may promote persistent immune suppression, a hallmark of chronic
454 critical illness and poor sepsis recovery.[5,16] Conversely, sex-biased promoter accessibility could
455 underlie known disparities in sepsis outcomes between males and females.[18] These mechanistic
456 insights may guide future strategies to therapeutically reprogram MDSCs using epigenetic
457 modulators such as histone deacetylase (HDAC) inhibitors, bromodomain inhibitors, or DNA
458 methyltransferase inhibitors, many of which are already being explored in oncologic and
459 inflammatory contexts.[7,26]
460
461 Moreover, promoter classes defined here could serve as biomarkers of MDSC-state or targets for
462 selective modulation. For instance, genes in Classes 1-3 may be used to identify actively
463 suppressive MDSCs post-sepsis, while Class 8 promoters might be harnessed to identify aged
464 immune populations with impaired regulatory function. The stability of Class 9 loci suggests they
465 may serve as internal controls or indicators of MDSC identity in future epigenetic studies.
466

467 Our findings provide mechanistic insight into how sepsis may drive divergent epigenetic fates in
468 MDSCs that reflect hallmarks of both trained immunity and tolerance. The persistent chromatin
469 accessibility observed at Class 1-3 promoters (e.g., *S100a9*, *Nos2*, *S100a8*), particularly in older
470 or female hosts, suggests a form of innate immune training, where prior inflammatory exposure
471 leaves a molecular imprint that primes these loci for rapid reactivation. This is consistent with
472 studies showing that chromatin remodeling at promoters of inflammatory genes underlies the
473 trained phenotype in monocytes and macrophages (reviewed in[48]). Conversely, the selective
474 silencing of promoters in Classes 6-8, including key regulatory genes such as *Cd274* and *Il10*,
475 supports the emergence of an epigenetic tolerance program, particularly in aged MDSCs. These
476 loci become refractory to activation despite hypomethylation, implicating nucleosome
477 repositioning and chromatin compaction as dominant suppressive mechanisms. The coexistence
478 of both accessibility gains and repressive remodeling across promoter classes indicates that sepsis
479 induces a divergent epigenetic landscape in MDSCs, poising some genes for increased
480 responsiveness while silencing others. These dual trajectories may underlie the paradoxical state
481 of immune hyperinflammation coupled with functional suppression seen in sepsis survivors and
482 reflect an imprint of the inflammatory milieu on the myeloid epigenome that varies by age and
483 sex.
484
485 *Limitations*
486 This study focused on a pre-selected set of immune and MDSC-relevant promoters, limiting
487 discovery of unanticipated regulatory regions or enhancer-driven transcription. Additionally,
488 while we profiled $Gr1^{+}CD11b^{+}$ splenocytes, these include multiple MDSC subtypes and
489 potentially other myeloid cells. Although scRNA-seq helped disaggregate subtype-specific effects,

490 future studies using single-cell epigenomics (e.g., scATAC-seq or scCUT&Tag) could more finely
491 resolve MDSC heterogeneity.[49] Finally, the MAPit-FENGC dataset provides high-resolution data
492 at selected promoters—the approach can be readily extended to capture distal regulatory elements,
493 which may play significant roles in aging-related immune dysfunction.
494

495 **Resource Availability**

496 Requests for further information and resources should be directed to and will be fulfilled by the
497 lead contact, Michael Kladde, PhD (kladde@ufl.edu). This study did not generate new unique
498 reagents. Data pending submission to GEO.
499

500 **Acknowledgments**
501
502 This work was supported, in part, by the following grants:
503 National Institutes of Health T32GM008721, T32HL160491, RF1NS128626, R21AG087039
504 Department of Defense, Defense Threat Reduction Agency Grant 11912108
505

506 **Author Contributions**
507 Conceptualization: MPK, PAE
508 Formal analysis: RLB, DBD, MPLG, JOB, MZ, FX, GC, RM, MPK
509 Funding acquisition: PAE, MPK, GC, PC
510 Investigation: MPLG, JOB, MPK
511 Methodology: MPK, MZ
512 Project administration: MPK
513 Supervision: PAE, LLM, RM, MPK
514 Visualization: RM, MPK
515 Writing – original draft: AMC, DBD, CER, PAE, RM, MPK
516 Writing – review & editing: CER, AMC, MH, MPG, JOB, RLB, LB, AMM, FX, GC, SMW, CEM,
517 LLM, PAE, RM, MPK
518

519 **Declaration of Interests**

MPK, the corresponding author, and MZ are co-inventors of pending patent application US18/551,004 (Methods and kits for targeted cleavage and enrichment of nucleic acids for high-throughput analyses of user-defined genomic regions) for FENGC and MAPit-FENGC. The remaining authors declare no competing interests.

524 **FIGURE LEGENDS**

525 **Figure 1. Class 1 and 2 promoters exhibit robust sepsis-induced chromatin accessibility, with**
526 **age- and sex-specific differences and partial demethylation across MDSC subsets**

527 (A) Representative single-molecule MAPit-FENGC plots for selected Class 1 promoters, showing
528 simultaneous profiling of endogenous CpG methylation (HCG, left of each pair of panels, red) and
529 *in vitro* GpC methylation (GCH, right of each pair, yellow) in Gr1$^+$ MDSCs from four experimental
530 groups: Young Naïve, Young Sepsis, Older Naïve, and Older Sepsis, all from female mice. Each
531 horizontal line represents a unique DNA molecule, with the total number indicated on the y-axis.
532 Black and gray marks denote methylated cytosines, while yellow marks indicate unmethylated
533 (open or accessible) cytosines. Promoters are organized by gene and condition; Class 1 promoters
534 were defined by consistent nucleosome-free region (NFR) formation (highlighted by blue boxes)
535 in all septic groups, which co-localizes with the TSS (arrow). The black bar on top of the base pair
536 scale is the size of a nucleosome particle (147 bp). Particularly robust NFRs are observed in *Older*
537 *Sepsis* conditions, especially in females. (B) Group-averaged chromatin accessibility (GpC
538 methylation) across the same *S100a9* region, plotted separately for males (left) and females (right).
539 (C) Group-averaged endogenous CpG methylation levels across the *S100a9* promoter. (D-F)
540 Equivalent plots for the Class 2 promoter genes *Cxcr2* in Gr1$^+$ MDSCs.

541

542 **Figure 2. Class 3 promoters are consistently accessible in sepsis across all age and sex groups,**
543 **and Class 4 promoters are activated by sepsis in females only**

544 (A) Single-molecule MAPit-FENGC plots for Class 3 genes (e.g., *Mmp8*), showing HCG (left)
545 and GCH (right) signals across Young/Older Female MDSCs. Sepsis induces NFRs in all septic
546 conditions, regardless of age. The figure is annotated as in Figure 1. (B) Group-averaged chromatin

547 accessibility (GpC methylation) across the same region, plotted separately for males (left) and
548 females (right). (C) Group-averaged endogenous CpG methylation levels across the promoter. (D-
549 F) Equivalent plots for the Class 4 promoter *Fyb.* The additional green boxes in (D) highlight areas
550 of protection against the GpC DNA methyltransferase chromatin probe, which accompanies NFR
551 formation in MDSCs from female septic mice. Red shading in (F) indicates sequences that contain
552 CCG sites, an off-target specificity of the GpC enzyme, which therefore do not reflect *bona fide*
553 CpG methylation.
554
555 **Figure 3. Class 5-7 promoters possess varying levels of DNA methylation but are all packaged**
556 **into arrays of positioned nucleosomes, where linkers lose accessibility in Older Sepsis only**
557 (A) MAPit-FENGC plots of *Lyz1* showing no detectable NFRs in any condition across MDSCs
558 from young/older female mice. HCG and GCH signals indicate high methylation and random
559 nucleosome positioning. The figure is annotated as in Figures 1 and 2. (B) Group-averaged
560 chromatin accessibility (GpC methylation) across the same region, plotted separately for males
561 (left) and females (right). (C) Group-averaged endogenous CpG methylation levels across the
562 promoter. (D-F) Equivalent plots for the Class 6 *Serpine1* promoter. (G-I) Equivalent plots for the
563 Class 7 *Vcan* promoter.
564
565 **Figure 4. Class 8 promoters constitutively harbor well-defined NFRs across all conditions,**
566 **which partially lose accessibility specifically in Female Older Sepsis**
567 (A) HCG and GCH plots for *Cd274* promoter show prominent NFRs across all conditions. The
568 figure is annotated as in Figures 1 and 2. (B) Group-averaged chromatin accessibility (GpC
569 methylation) across the same region, plotted separately for males (left) and females (right). (C)

570 Group-averaged endogenous CpG methylation levels across the promoter. (D-F) Equivalent plots
571 for *Nfkbiz* promoter.
572
573 **Figure 5. Class 9 promoters are constitutively open in sepsis**
574 (A) HCG and GCH plots for the *Tet2* promoter show strong, stable NFRs in all female MDSCs.
575 The figure is annotated as in Figures 1 and 2. (B) Group-averaged chromatin accessibility (GpC
576 methylation) across the same region, plotted separately for males (left) and females (right). No
577 group-averaged endogenous CpG methylation in shown because all HCG sites are CCG.
578
579 **Figure 6. Class 1 and Class 3 genes show consistent sepsis-induced transcriptional activation**
580 **across MDSC subsets**
581 Bar plots $\log_2$ fold change in expression for *S100a9* (Class 1) and *S100a8* (Class 3) across E-
582 MDSC, M-MDSC, and PMN-MDSC populations (conditions and comparisons as labeled) derived
583 from single-cell RNA-sequencing analysis of splenic $Cd11b^+$ $Gr1^+$ cells.
584
585 **Figure 7. Expression of Class 7, Class 8 and Class 9 genes across MDSC subtypes reveals**
586 **repression and age-dependent silencing**
587 Bar plots depict $\log_2$ fold change in gene expression (conditions and comparisons as labeled) for
588 *Ccl5* (Class 7), *Nfkbiz* (Class 8) and *Tet2* (Class 9),derived from single-cell RNA-seq analysis of
589 splenic $Cd11b^+$ $Gr1^+$ cells. Data are shown separately for early MDSCs (E-MDSC), monocytic
590 MDSCs (M-MDSC), and polymorphonuclear MDSCs (PMN-MDSC).
591
592

593 **Methods**

594 **Experimental Model**

595 ***Animals***

596 Young and older adult female (50%) and male (50%) mice underwent our intra-abdominal sepsis
597 model of cecal ligation and puncture (CLP) followed by daily chronic stress (DCS).
598 Approximately eight to 12 mice were used per experimental group. Mice were euthanized seven
599 days post CLP + DCS. Experimental mice were euthanized in compliance with predetermined
600 IACUC Body Condition Score (BCS) criteria. A modification to this included the following:
601 greater than or equal to 20% weight loss from baseline or from age-matched controls if the animals
602 are still growing during the study or greater than or equal to 20% weight loss from baseline in
603 older mice who have a BCS of greater than 2 in the first five days after CLP, or greater than 40%
604 weight loss from baseline in older mice with a BCS greater than 2 after five days following CLP.
605 Based on these criteria, no mice had to be euthanized for excessive weight loss during the course
606 of the study.

607

608 ***Intra-Abdominal Sepsis Model***

609 CLP was conducted under isoflurane anesthesia we have previously described[50]. The
610 cecum was ligated 1 cm from its tip and a 22- or 25-gauge needle was used to puncture the cecum
611 depending on the desired experimental mortality. Buprenorphine analgesia was provided for 48
612 hours post surgery. Antibiotics (imipenem monohydrate; 25 mg/kg diluted in 1 mL 0.9% sodium
613 chloride [NaCl]) were administered two hours post-CLP then continued for 72 hours. DCS was
614 conducted as previously described[51]. Briefly, this involved placing mice in weighted plexiglass
615 animal restraint holders (Kent Scientific, Torrington, CT) for two hours daily starting the day after

616 CLP. The purpose was to simulate the ICU environment, where patients are often bedbound with
617 limited mobility. MDSC were isolated using a $CD11b^{+}Gr1^{+}$ isolation (EasySep™ Mouse MDSC
618 (CD11b+Gr1+) Isolation Kit, StemCell, Cambridge, MA, USA) according to manufacturer's
619 instructions and as we have described previously[21].
620
621 **Methods Details**
622 ***Single-cell RNA sequencing (scRNA-seq) analysis***
623 Splenocytes were obtained and counts were quantified using a Cellometer™ Auto 2000 Cell
624 Viability Counter (Nexcelom Bioscience, Lawrence, MA). One million cells with a minimum of
625 85% cell viability were obtained for scRNAseq using 10X Genomics chemistry (Chromium X
626 instrument, Pleasonton, CA). as described in the companion paper (Rodhouse *et al*).
627
628 ***Methyltransferase Accessibility Protocol for Individual Templates combined with Flap-Enabled***
629 ***Next-Generation Capture (MAPit-FENGC) epigenetic analysis.***
630 MAPit-FENGC is a validated method that allows for simultaneous single-molecular level analysis
631 of methylation and accessibility at target promoter and enhancer regions[27]**.** One million cells from
632 each mouse were washed with ice-cold PBS, pH 7.2. Cells were centrifuged at 1,000 *x g* for five
633 min then washed in ice-cold cell resuspension buffer (20 mM HEPES pH 7.5, 70 mM NaCl, 0.25
634 mM EDTA pH 8.0, 0.5 mM EGTA pH 8.0, 0.5% glycerol, with freshly supplemented 10 mM DTT
635 and 0.25 mM PMSF). Cells were centrifuged at 1,000 *x g* for five min before being resuspended
636 with 92 μL of resuspension buffer with 0.5 % digitonin. Cells were then stained with trypan blue
637 to ascertain 100 % permeabilization. The cells were then treated with 100 U M.CviPI GpC
638 methyltransferase (100 U / million cells; New England Biolabs, M0227B-HI) with fresh 160 160

639 μM S-adenosyl-L-methionine for 15 min at 37°C. The reaction was terminated using an equal
640 volume of 10 mM EDTA, 100 mM NaCl, and 1% (w/v) SDS followed by a quick vortex at medium
641 speed. The nuclei were treated with 100 μg/ml RNase A for 30 min at 37°C followed with 100
642 μg/ml proteinase K treatment at 50°C overnight. Extraction of genomic DNA was conducted using
643 phenol-chloroform-isoamyl alcohol (25:24:1, v/v) phase separation, which was followed by
644 ethanol precipitation, then resuspension in molecular-grade H_2O. The full FENGC methodology
645 can be found at Zhou et al. (2022)[27]. Target gene promoters and enhancers were located using the
646 transcription start site (TSS) region and encode annotations from the mm10 genome assembly.
647 Flap oligos 1 and 2 as well as the nested oligos 3 are catalogued in **Supplementary Material 1**.
648 All three oligos (4 nmole each) were ordered as 0.3-mL each as salt-free oligos in 96 well format
649 (Eurofins Genomics, KY, USA). Purified amplicons were submitted to the University of Florida
650 Interdisciplinary Center for Biotechnology Research (UF-ICBR, RRID:SCR_019152) for SMRT
651 bell library construction. Sequencing was run on PacBio SEQUEL IIe (City, State) instrument by
652 UF-ICBR. The library pool was loaded at 120 pM, using diffusion loading and 20- to 30- h movies
653 with HiFi generation and demultiplexing. Sequencing Kit 2.0 (PacBio, 101-389-001) and
654 Instrument Chemistry Bundle Version 11.0 were used with all other steps being performed using
655 recommended protocol by the PacBio sequencing calculator. For epigenetic analysis, high-fidelity
656 circular consensus sequencing (CCS) was generated using default parameters except for a setting
657 of ≥ 5 single polymerase read passes. CCS reads were aligned to the reference sequences using
658 the python reAminator pipeline[52]. Cut-offs to 95% conversion rate and 95% length of reference
659 sequences alignments were applied. To distinguish endogenous CG methylation and M.CviPI-
660 probed GC methylation, the unambiguously GCG sites were removed from calculation of HCG
661 and GCH methylation (where H is A, C, or T). Averaged heatmaps were constructed based on

662 averaged percent HCG/GCH per nucleotide post-methylscaper analysis[53]. A total of 180 primers
663 for selected promoter and enhancer regions of immune and trauma-related genes (**Supplemental**
664 **Material 1**) were used to concurrently profile chromatin accessibility and methylation. To assess
665 global epigenetic differences in $CD11b^{+}$ $Gr1^{+}$ MDSCs isolated from murine spleens, we used three
666 types of data matrices: (1) endogenous CpG methylation (HCG sites), (2) GpC methylation
667 representing chromatin accessibility (GCH sites), and (3) combined HCG + GCH profiles. For
668 each sample, a matrix of percent methylation across covered sites was generated and filtered to
669 retain loci with ≥25 informative reads. Principal component analysis (PCA) was conducted using
670 base R's prcomp() function without imputation. After quality filtering, each promoter target was
671 filtered for fewer than 25 reads. Targets were not used in the PCAs if < 2 samples had data passing
672 the filter.

673

674 **REFERENCES**

675 1. Singer, M., Deutschman, C.S., Seymour, C.W., Shankar-Hari, M., Annane, D., Bauer, M., Bellomo, R.,
676 Bernard, G.R., Chiche, J.D., Coopersmith, C.M., et al. (2016). The Third International Consensus
677 Definitions for Sepsis and Septic Shock (Sepsis-3). Jama *315*, 801–810. 10.1001/jama.2016.0287.

678 2. Rhee, C., Dantes, R., Epstein, L., Murphy, D.J., Seymour, C.W., Iwashyna, T.J., Kadri, S.S., Angus, D.C.,
679 Danner, R.L., Fiore, A.E., et al. (2017). Incidence and Trends of Sepsis in US Hospitals Using Clinical vs
680 Claims Data, 2009-2014. Jama *318*, 1241–1249. 10.1001/jama.2017.13836.

681 3. Hollenbeak, C.S., Henning, D.J., Geeting, G.K., Ledeboer, N.A., Faruqi, I.A., Pierce, C.G., Thomas, C.B.,
682 and O'Neal, H.R., Jr. (2023). Costs and Consequences of a Novel Emergency Department Sepsis
683 Diagnostic Test: The IntelliSep Index. Crit Care Explor *5*, e0942. 10.1097/CCE.0000000000000942.

684 4. Herran-Monge, R., Muriel-Bombin, A., Garcia-Garcia, M.M., Merino-Garcia, P.A., Martinez-Barrios,
685 M., Andaluz, D., Ballesteros, J.C., Dominguez-Berrot, A.M., Moradillo-Gonzalez, S., Macias, S., et al.
686 (2019). Epidemiology and Changes in Mortality of Sepsis After the Implementation of Surviving Sepsis
687 Campaign Guidelines. J Intensive Care Med *34*, 740–750. 10.1177/0885066617711882.

688 5. Darden, D.B., Brakenridge, S.C., Efron, P.A., Ghita, G.L., Fenner, B.P., Kelly, L.S., Mohr, A.M., Moldawer,
689 L.L., and Moore, F.A. (2021). Biomarker Evidence of the Persistent Inflammation, Immunosuppression
690 and Catabolism Syndrome (PICS) in Chronic Critical Illness (CCI) After Surgical Sepsis. Ann Surg *274*,
691 664–673. 10.1097/SLA.0000000000005067.

692 6. Brakenridge, S.C., Efron, P.A., Cox, M.C., Stortz, J.A., Hawkins, R.B., Ghita, G., Gardner, A., Mohr, A.M.,
693 Anton, S.D., Moldawer, L.L., and Moore, F.A. (2019). Current Epidemiology of Surgical Sepsis:
694 Discordance Between Inpatient Mortality and 1-year Outcomes. Ann Surg *270*, 502–510.
695 10.1097/sla.0000000000003458.

696 7. Polcz, V.E., Barrios, E.L., Larson, S.D., Efron, P.A., and Rincon, J.C. (2024). Charting the course for
697 improved outcomes in chronic critical illness: therapeutic strategies for persistent inflammation,
698 immunosuppression, and catabolism syndrome (PICS). Br J Anaesth *133*, 260–263.
699 10.1016/j.bja.2024.05.005.

700 8. Gabrilovich, D.I., Bronte, V., Chen, S.H., Colombo, M.P., Ochoa, A., Ostrand-Rosenberg, S., and
701 Schreiber, H. (2007). The terminology issue for myeloid-derived suppressor cells. Cancer Res *67*, 425;
702 author reply 426. 10.1158/0008-5472.CAN-06-3037.

703 9. Veglia, F., Sanseviero, E., and Gabrilovich, D.I. (2021). Myeloid-derived suppressor cells in the era of
704 increasing myeloid cell diversity. Nat Rev Immunol *21*, 485–498. 10.1038/s41577-020-00490-y.

705 10. Mira, J.C., Gentile, L.F., Mathias, B.J., Efron, P.A., Brakenridge, S.C., Mohr, A.M., Moore, F.A., and
706 Moldawer, L.L. (2017). Sepsis Pathophysiology, Chronic Critical Illness, and Persistent Inflammation-
707 Immunosuppression and Catabolism Syndrome. Crit Care Med *45*, 253–262.
708 10.1097/CCM.0000000000002074.

709 11. Uhel, F., Azzaoui, I., Gregoire, M., Pangault, C., Dulong, J., Tadie, J.M., Gacouin, A., Camus, C., Cynober,
710 L., Fest, T., et al. (2017). Early Expansion of Circulating Granulocytic Myeloid-derived Suppressor Cells
711 Predicts Development of Nosocomial Infections in Patients with Sepsis. Am J Respir Crit Care Med *196*,
712 315–327. 10.1164/rccm.201606-1143OC.

713 12. Mathias, B., Delmas, A.L., Ozrazgat-Baslanti, T., Vanzant, E.L., Szpila, B.E., Mohr, A.M., Moore, F.A.,
714 Brakenridge, S.C., Brumback, B.A., Moldawer, L.L., et al. (2017). Human Myeloid-derived Suppressor

715 Cells are Associated With Chronic Immune Suppression After Severe Sepsis/Septic Shock. Ann Surg
716 *265*, 827–834. 10.1097/SLA.0000000000001783.

717 13. Barrios, E.L., Leary, J.R., Darden, D.B., Rincon, J.C., Willis, M., Polcz, V.E., Gillies, G.S., Munley, J.A.,
718 Dirain, M.L., Ungaro, R., et al. (2024). The post-septic peripheral myeloid compartment reveals
719 unexpected diversity in myeloid-derived suppressor cells. Front Immunol *15*, 1355405.
720 10.3389/fimmu.2024.1355405.

721 14. Darden, D.B., Bacher, R., Brusko, M.A., Knight, P., Hawkins, R.B., Cox, M.C., Dirain, M.L., Ungaro, R.,
722 Nacionales, D.C., Rincon, J.C., et al. (2021). Single-Cell RNA-seq of Human Myeloid-Derived Suppressor
723 Cells in Late Sepsis Reveals Multiple Subsets With Unique Transcriptional Responses: A Pilot Study.
724 Shock *55*, 587–595. 10.1097/SHK.0000000000001671.

725 15. Hollen, M.K., Stortz, J.A., Darden, D., Dirain, M.L., Nacionales, D.C., Hawkins, R.B., Cox, M.C., Lopez,
726 M.C., Rincon, J.C., Ungaro, R., et al. (2019). Myeloid-derived suppressor cell function and epigenetic
727 expression evolves over time after surgical sepsis. Crit Care *23*, 355. 10.1186/s13054-019-2628-x.

728 16. Efron, P.A., Brakenridge, S.C., Mohr, A.M., Barrios, E.L., Polcz, V.E., Anton, S., Ozrazgat-Baslanti, T.,
729 Bihorac, A., Guirgis, F., Loftus, T.J., et al. (2023). The persistent inflammation, immunosuppression,
730 and catabolism syndrome 10 years later. J Trauma Acute Care Surg *95*, 790–799.
731 10.1097/TA.0000000000004087.

732 17. Efron, P.A., Darden, D.B., Li, E.C., Munley, J., Kelly, L., Fenner, B., Nacionales, D.C., Ungaro, R.F., Dirain,
733 M.L., Rincon, J., et al. (2022). Sex differences associate with late microbiome alterations after murine
734 surgical sepsis. J Trauma Acute Care Surg *93*, 137–146. 10.1097/ta.0000000000003599.

735 18. Rani, A., Barter, J., Kumar, A., Stortz, J.A., Hollen, M., Nacionales, D., Moldawer, L.L., Efron, P.A., and
736 Foster, T.C. (2022). Influence of age and sex on microRNA response and recovery in the hippocampus
737 following sepsis. Aging (Albany NY) *14*, 728–746. 10.18632/aging.203868.

738 19. Mankowski, R.T., Thomas, R.M., Darden, D.B., Gharaibeh, R.Z., Hawkins, R.B., Cox, M.C., Apple, C.,
739 Nacionales, D.C., Ungaro, R.F., Dirain, M.L., et al. (2021). Septic Stability? Gut Microbiota in Young
740 Adult Mice Maintains Overall Stability After Sepsis Compared to Old Adult Mice. Shock *55*, 519–525.
741 10.1097/shk.0000000000001648.

742 20. Mankowski, R.T., Anton, S.D., Ghita, G.L., Brumback, B., Cox, M.C., Mohr, A.M., Leeuwenburgh, C.,
743 Moldawer, L.L., Efron, P.A., Brakenridge, S.C., and Moore, F.A. (2020). Older Sepsis Survivors Suffer
744 Persistent Disability Burden and Poor Long-Term Survival. J Am Geriatr Soc *68*, 1962–1969.
745 10.1111/jgs.16435.

746 21. Stortz, J.A., Hollen, M.K., Nacionales, D.C., Horiguchi, H., Ungaro, R., Dirain, M.L., Wang, Z., Wu, Q.,
747 Wu, K.K., Kumar, A., et al. (2019). Old Mice Demonstrate Organ Dysfunction as well as Prolonged
748 Inflammation, Immunosuppression, and Weight Loss in a Modified Surgical Sepsis Model. Crit Care
749 Med *47*, e919–e929. 10.1097/ccm.0000000000003926.

750 22. Barter, J., Kumar, A., Stortz, J.A., Hollen, M., Nacionales, D., Efron, P.A., Moldawer, L.L., and Foster,
751 T.C. (2019). Age and Sex Influence the Hippocampal Response and Recovery Following Sepsis. Mol
752 Neurobiol *56*, 8557–8572. 10.1007/s12035-019-01681-y.

753 23. Brakenridge, S.C., Efron, P.A., Stortz, J.A., Ozrazgat-Baslanti, T., Ghita, G., Wang, Z., Bihorac, A., Mohr,
754 A.M., Brumback, B.A., Moldawer, L.L., and Moore, F.A. (2018). The impact of age on the innate
755 immune response and outcomes after severe sepsis/septic shock in trauma and surgical intensive care
756 unit patients. J Trauma Acute Care Surg *85*, 247–255. 10.1097/TA.0000000000001921.

757 24. Raymond, S.L., Lopez, M.C., Baker, H.V., Larson, S.D., Efron, P.A., Sweeney, T.E., Khatri, P., Moldawer,
758 L.L., and Wynn, J.L. (2017). Unique transcriptomic response to sepsis is observed among patients of
759 different age groups. PLoS One *12*, e0184159. 10.1371/journal.pone.0184159.

760 25. Nacionales, D.C., Szpila, B., Ungaro, R., Lopez, M.C., Zhang, J., Gentile, L.F., Cuenca, A.L., Vanzant, E.,
761 Mathias, B., Jyot, J., et al. (2015). A Detailed Characterization of the Dysfunctional Immunity and
762 Abnormal Myelopoiesis Induced by Severe Shock and Trauma in the Aged. J Immunol *195*, 2396–2407.
763 10.4049/jimmunol.1500984.

764 26. Gjerstorff, M.F. (2023). Epigenetic targeting of myeloid-derived suppressor cells: time to move into
765 infectious diseases? Front Immunol *14*, 1247715. 10.3389/fimmu.2023.1247715.

766 27. Zhou, M., Nabilsi, N.H., Wang, A., Gauthier, M.-P.L., Murray, K.O., Azari, H., Owens, W.S., Newman,
767 J.R.B., Pardo-Palacios, F.J., Conesa, A., et al. (2022–11–09). Flap-enabled next-generation capture
768 (FENGC): precision targeted single-molecule profiling of epigenetic heterogeneity, chromatin
769 dynamics, and genetic variation. bioRxiv. 10.1101/2022.11.08.515732.

770 28. Knight, P., Gauthier, M.L., Pardo, C.E., Darst, R.P., Kapadia, K., Browder, H., Morton, E., Riva, A., Kladde,
771 M.P., and Bacher, R. (2021). Methylscaper: an R/Shiny app for joint visualization of DNA methylation
772 and nucleosome occupancy in single-molecule and single-cell data. Bioinformatics *37*, 4857–4859.
773 10.1093/bioinformatics/btab438.

774 29. von Wulffen, M., Luehrmann, V., Robeck, S., Russo, A., Fischer-Riepe, L., van den Bosch, M., van Lent,
775 P., Loser, K., Gabrilovich, D.I., Hermann, S., et al. (2023). S100A8/A9-alarmin promotes local myeloid-
776 derived suppressor cell activation restricting severe autoimmune arthritis. Cell Rep *42*, 113006.
777 10.1016/j.celrep.2023.113006.

778 30. Davison, L.M., Alberto, A.A., Dand, H.A., Keller, E.J., Patt, M., Khan, A., Dvorina, N., White, A., Sakurai,
779 N., Liegl, L.N., et al. (2021). S100a9 Protects Male Lupus-Prone NZBWF1 Mice From Disease
780 Development. Front Immunol *12*, 681503. 10.3389/fimmu.2021.681503.

781 31. Bullock, K., and Richmond, A. (2021). Suppressing MDSC Recruitment to the Tumor Microenvironment
782 by Antagonizing CXCR2 to Enhance the Efficacy of Immunotherapy. Cancers (Basel) *13*.
783 10.3390/cancers13246293.

784 32. Santibanez, J.F. (2025). Myeloid-Derived Suppressor Cells: Implications in Cancer Immunology and
785 Immunotherapy. Front Biosci (Landmark Ed) *30*, 25203. 10.31083/FBL25203.

786 33. Wang, S., Zhao, X., Wu, S., Cui, D., and Xu, Z. (2023). Myeloid-derived suppressor cells: key
787 immunosuppressive regulators and therapeutic targets in hematological malignancies. Biomark Res
788 *11*, 34. 10.1186/s40364-023-00475-8.

789 34. Ibrahim, A.A., Fujimura, T., Uno, T., Terada, T., Hirano, K.I., Hosokawa, H., Ohta, A., Miyata, T., Ando,
790 K., and Yahata, T. (2024). Plasminogen activator inhibitor-1 promotes immune evasion in tumors by
791 facilitating the expression of programmed cell death-ligand 1. Front Immunol *15*, 1365894.
792 10.3389/fimmu.2024.1365894.

793 35. Brune, J.E., Chang, M.Y., Altemeier, W.A., and Frevert, C.W. (2021). Type I Interferon Signaling
794 Increases Versican Expression and Synthesis in Lung Stromal Cells During Influenza Infection. J
795 Histochem Cytochem *69*, 691–709. 10.1369/00221554211054447.

796 36. Chang, M.Y., Tanino, Y., Vidova, V., Kinsella, M.G., Chan, C.K., Johnson, P.Y., Wight, T.N., and Frevert,
797 C.W. (2014). A rapid increase in macrophage-derived versican and hyaluronan in infectious lung
798 disease. Matrix Biol *34*, 1–12. 10.1016/j.matbio.2014.01.011.

799 37. Yaseen, M.M., Abuharfeil, N.M., Darmani, H., and Daoud, A. (2020). Mechanisms of immune
800 suppression by myeloid-derived suppressor cells: the role of interleukin-10 as a key
801 immunoregulatory cytokine. Open Biol *10*, 200111. 10.1098/rsob.200111.

802 38. Wang, J.C., and Sun, L. (2022). PD-1/PD-L1, MDSC Pathways, and Checkpoint Inhibitor Therapy in Ph(-
803) Myeloproliferative Neoplasm: A Review. Int J Mol Sci *23*. 10.3390/ijms23105837.

804 39. Jayakumar, A., and Bothwell, A.L.M. (2019). Functional Diversity of Myeloid-Derived Suppressor Cells:
805 The Multitasking Hydra of Cancer. J Immunol *203*, 1095–1103. 10.4049/jimmunol.1900500.

806 40. Groth, C., Hu, X., Weber, R., Fleming, V., Altevogt, P., Utikal, J., and Umansky, V. (2019).
807 Immunosuppression mediated by myeloid-derived suppressor cells (MDSCs) during tumour
808 progression. Br J Cancer *120*, 16–25. 10.1038/s41416-018-0333-1.

809 41. Jauch-Speer, S.L., Herrera-Rivero, M., Ludwig, N., Veras De Carvalho, B.C., Martens, L., Wolf, J., Imam
810 Chasan, A., Witten, A., Markus, B., Schieffer, B., et al. (2022). C/EBPdelta-induced epigenetic changes
811 control the dynamic gene transcription of S100a8 and S100a9. Elife *11*. 10.7554/eLife.75594.

812 42. Pappritz, K., Voss, I., El-Shafeey, M., and Van Linthout, S. (2025). Sex differences in age-related cardiac
813 and splenic S100A9 and NLRP3 expression. J Leukoc Biol. 10.1093/jleuko/qiaf031.

814 43. Stadtmann, A., and Zarbock, A. (2012). CXCR2: From Bench to Bedside. Front Immunol *3*, 263.
815 10.3389/fimmu.2012.00263.

816 44. Li, S., Feng, J., Wu, F., Cai, J., Zhang, X., Wang, H., Fetahu, I.S., Iwanicki, I., Ma, D., Hu, T., et al. (2020).
817 TET2 promotes anti-tumor immunity by governing G-MDSCs and CD8(+) T-cell numbers. EMBO Rep
818 *21*, e49425. 10.15252/embr.201949425.

819 45. Cai, Z., Kotzin, J.J., Ramdas, B., Chen, S., Nelanuthala, S., Palam, L.R., Pandey, R., Mali, R.S., Liu, Y.,
820 Kelley, M.R., et al. (2018). Inhibition of Inflammatory Signaling in Tet2 Mutant Preleukemic Cells
821 Mitigates Stress-Induced Abnormalities and Clonal Hematopoiesis. Cell Stem Cell *23*, 833–849 e835.
822 10.1016/j.stem.2018.10.013.

823 46. Barrios, E.L., Rincon, J.C., Willis, M., Polcz, V.E., Leary, J.R., Darden, D.B., Balch, J.A., Larson, S.D.,
824 Loftus, T.J., Mohr, A.M., et al. (2024). Transcriptomic Differences in Peripheral Monocyte Populations
825 in Septic Patients Based on Outcome. Shock *62*, 208–216. 10.1097/SHK.0000000000002379.

826 47. Balch, J.A., Chen, U.I., Liesenfeld, O., Starostik, P., Loftus, T.J., Efron, P.A., Brakenridge, S.C., Sweeney,
827 T.E., and Moldawer, L.L. (2023). Defining critical illness using immunological endotypes in patients
828 with and without sepsis: a cohort study. Crit Care *27*, 292. 10.1186/s13054-023-04571-x.

829 48. Sherwood, E.R., Burelbach, K.R., McBride, M.A., Stothers, C.L., Owen, A.M., Hernandez, A., Patil, N.K.,
830 Williams, D.L., and Bohannon, J.K. (2022). Innate Immune Memory and the Host Response to
831 Infection. J Immunol *208*, 785–792. 10.4049/jimmunol.2101058.

832 49. Rincon, J.C., Wang, D., Polcz, V.E., Barrios, E.L., Dirain, M.L., Ungaro, R.F., Nacionales, D.C., Zeumer-
833 Spataro, L., Xiao, F., Efron, P.A., et al. (2025). Innate immune training in the neonatal response to
834 sepsis. Molecular medicine *31*, 159. 10.1186/s10020-025-01179-5.

835 50. Nacionales, D.C., Gentile, L.F., Vanzant, E., Lopez, M.C., Cuenca, A., Cuenca, A.G., Ungaro, R., Li, Y.,
836 Baslanti, T.O., Bihorac, A., et al. (2014). Aged mice are unable to mount an effective myeloid response
837 to sepsis. J Immunol *192*, 612–622. 10.4049/jimmunol.1302109.

838 51. Bible, L.E., Pasupuleti, L.V., Gore, A.V., Sifri, Z.C., Kannan, K.B., and Mohr, A.M. (2015). Chronic
839 restraint stress after injury and shock is associated with persistent anemia despite prolonged

840 elevation in erythropoietin levels. J Trauma Acute Care Surg *79*, 91–96; discussion 96–97.
841 10.1097/TA.0000000000000686.

842 52. JR, S., MA, H., T, S., Y, K., CE, P., NH, N., RP, D., R, P., K, I., S, H., et al. (10/26/2015). High Fractional
843 Occupancy of a Tandem Maf Recognition Element and Its Role in Long-Range β-Globin Gene
844 Regulation - PubMed. Molecular and cellular biology *36*. 10.1128/MCB.00723-15.

845 53. P, K., ML, G., CE, P., RP, D., K, K., H, B., E, M., A, R., MP, K., and R, B. (12/11/2021). Methylscaper: an
846 R/Shiny app for joint visualization of DNA methylation and nucleosome occupancy in single-molecule
847 and single-cell data - PubMed. Bioinformatics (Oxford, England) *37*. 10.1093/bioinformatics/btab438.

848

Table 1. Gene Promoters Grouped by Epigenetic Class.

Epigenetic Class	Gene Promoters
1	*S100a9*
2	*Ccl3, Cxcr2, Il1rl2, Lcn2, Lgals9, Nos2, Ptgs2, Rnase2a*
3	*Mmp8, Ros1, S100a8*
4	*Fyb*
5	*Dab2, Emp1, F7, Lyz1, Mmp19, Pmp22, Retn, Serpina1a, Vnn1, Vsig4*
6	*Ambp, Ccl5, Cd9, Cxcl3, Fabp7, Fgr, Gpnmb, Kdm6b, Lgals2, Mmp9, Saa3, Serpine1, Sparc*
7	*Car4, Ccl17, Gprc5b, Htr2a, Igkv12-44, Igkv12-46, Igkv4-69 , Il10, Mt2, Plac8, S100a10, Stab1, Tmem176a, Tmem176a, Vcan*
8	*Atf6, Cd274, Hdac3, Il4ra, Nfkbiz, Vdr*
9	*Jun, Tet2, Stat3*

Figure 1

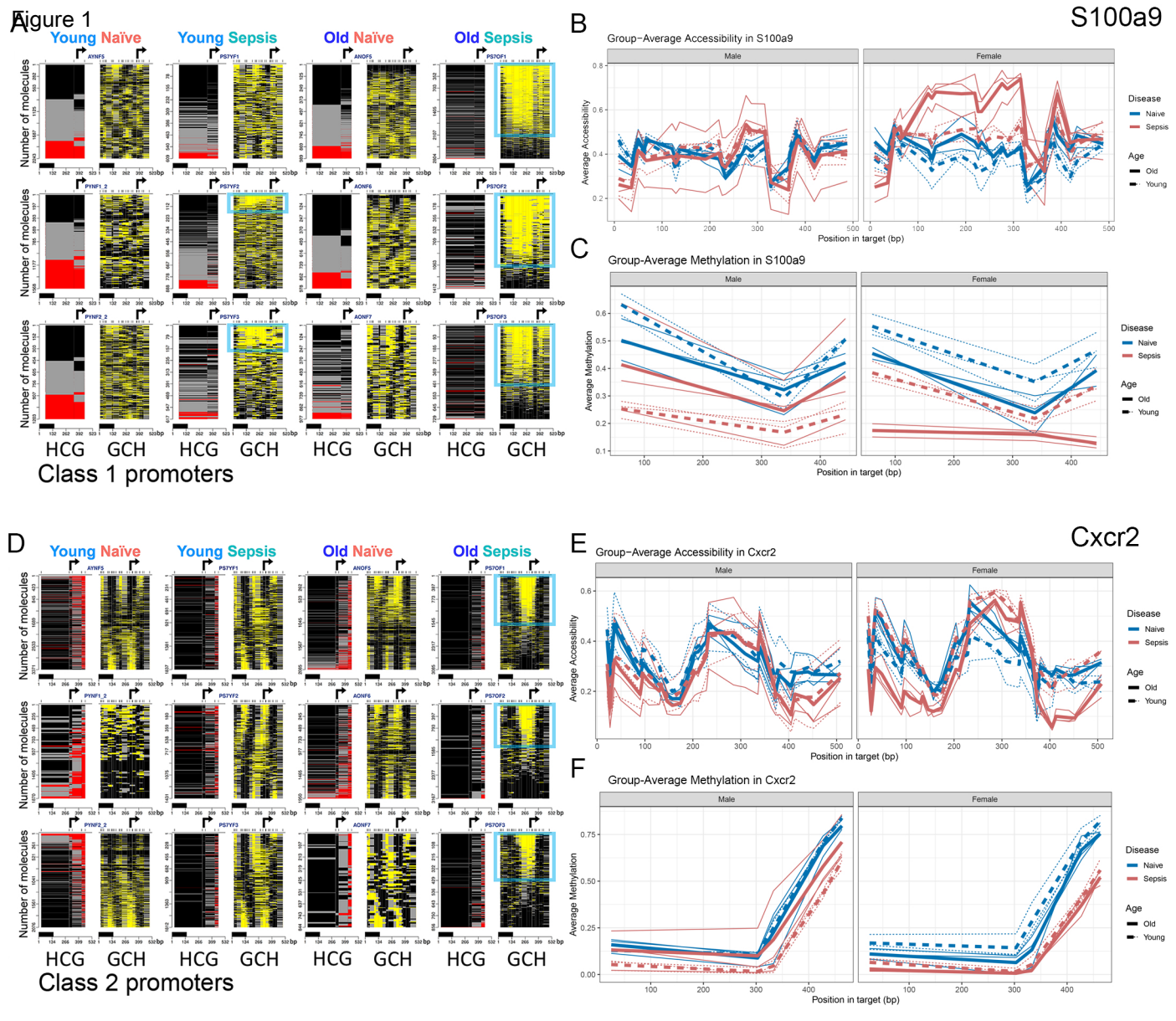
A
Young Naïve
Young Sepsis
Old Naïve
Old Sepsis
Number of molecules
HCG
GCH
Class 1 promoters
B
S100a9
Group-Average Accessibility in S100a9
Male
Female
Average Accessibility
Position in target (bp)
Disease
Naive
Sepsis
Age
Old
Young
C
Group-Average Methylation in S100a9
Average Methylation
D
Class 2 promoters
E
Cxcr2
Group-Average Accessibility in Cxcr2
F
Group-Average Methylation in Cxcr2

Figure 2

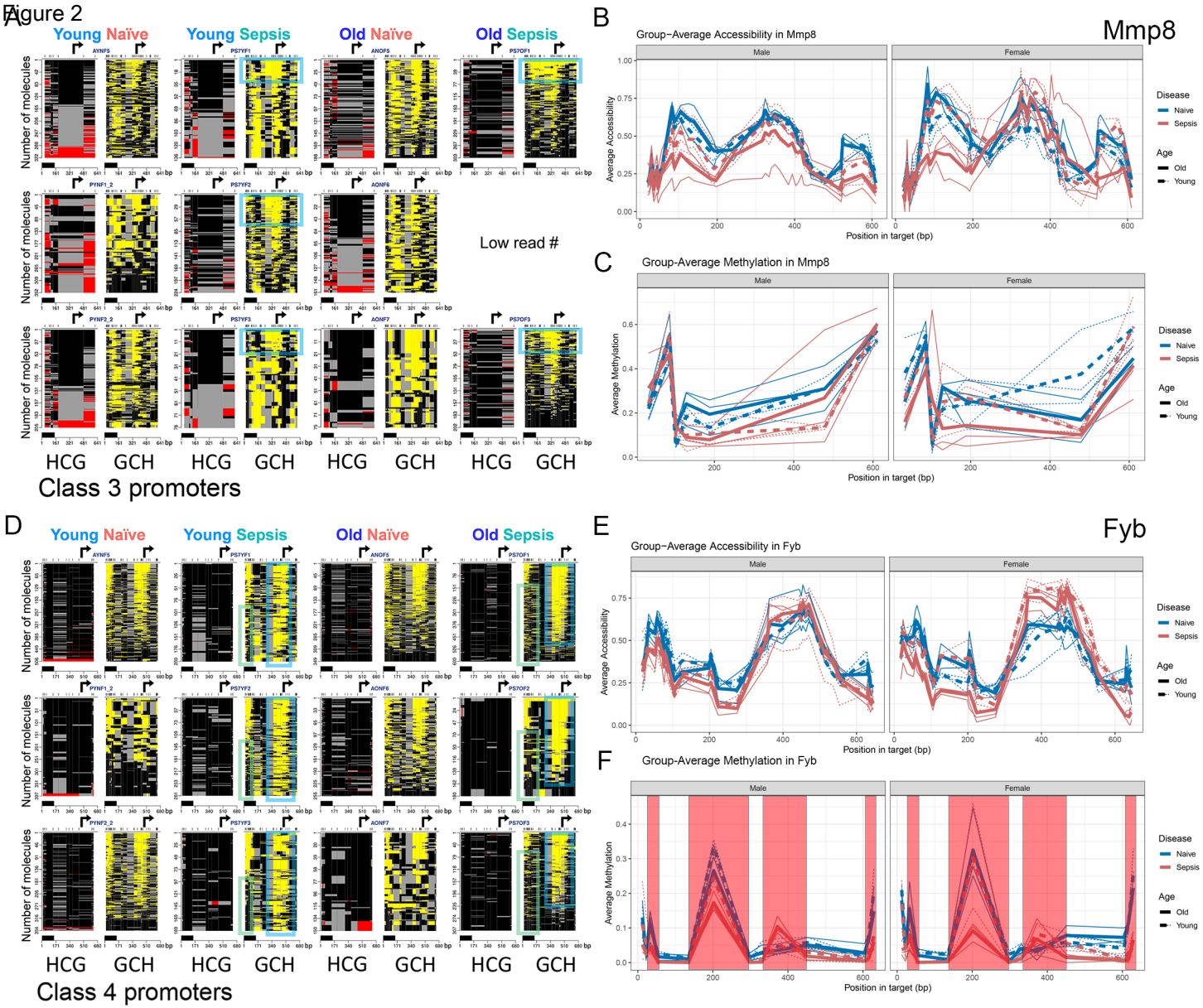
A
Young Naïve
Young Sepsis
Old Naïve
Old Sepsis
Number of molecules
Low read #
HCG
GCH
Class 3 promoters
B
Mmp8
Group−Average Accessibility in Mmp8
Male
Female
Average Accessibility
Position in target (bp)
Disease
Naive
Sepsis
Age
Old
Young
C
Group-Average Methylation in Mmp8
Average Methylation
D
Class 4 promoters
E
Fyb
Group−Average Accessibility in Fyb
F
Group-Average Methylation in Fyb

Figure 3

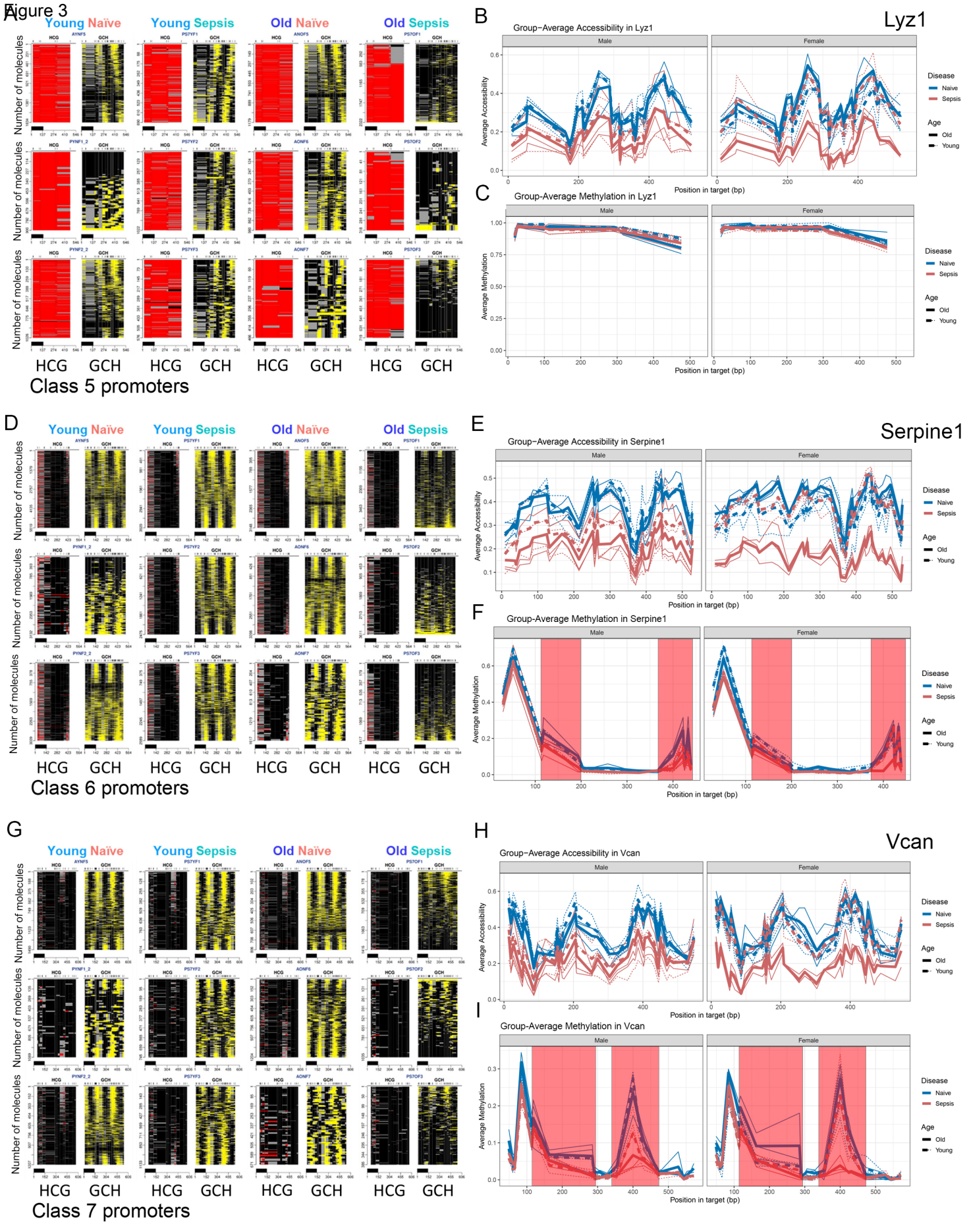
A
Young Naïve
Young Sepsis
Old Naïve
Old Sepsis
Number of molecules
HCG
GCH
Class 5 promoters
B
Lyz1
Group−Average Accessibility in Lyz1
Male
Female
Average Accessibility
Position in target (bp)
Disease
Naive
Sepsis
Age
Old
Young
C
Group-Average Methylation in Lyz1
Average Methylation
D
Class 6 promoters
E
Serpine1
Group−Average Accessibility in Serpine1
F
Group-Average Methylation in Serpine1
G
Class 7 promoters
H
Vcan
Group−Average Accessibility in Vcan
I
Group-Average Methylation in Vcan

Figure 4

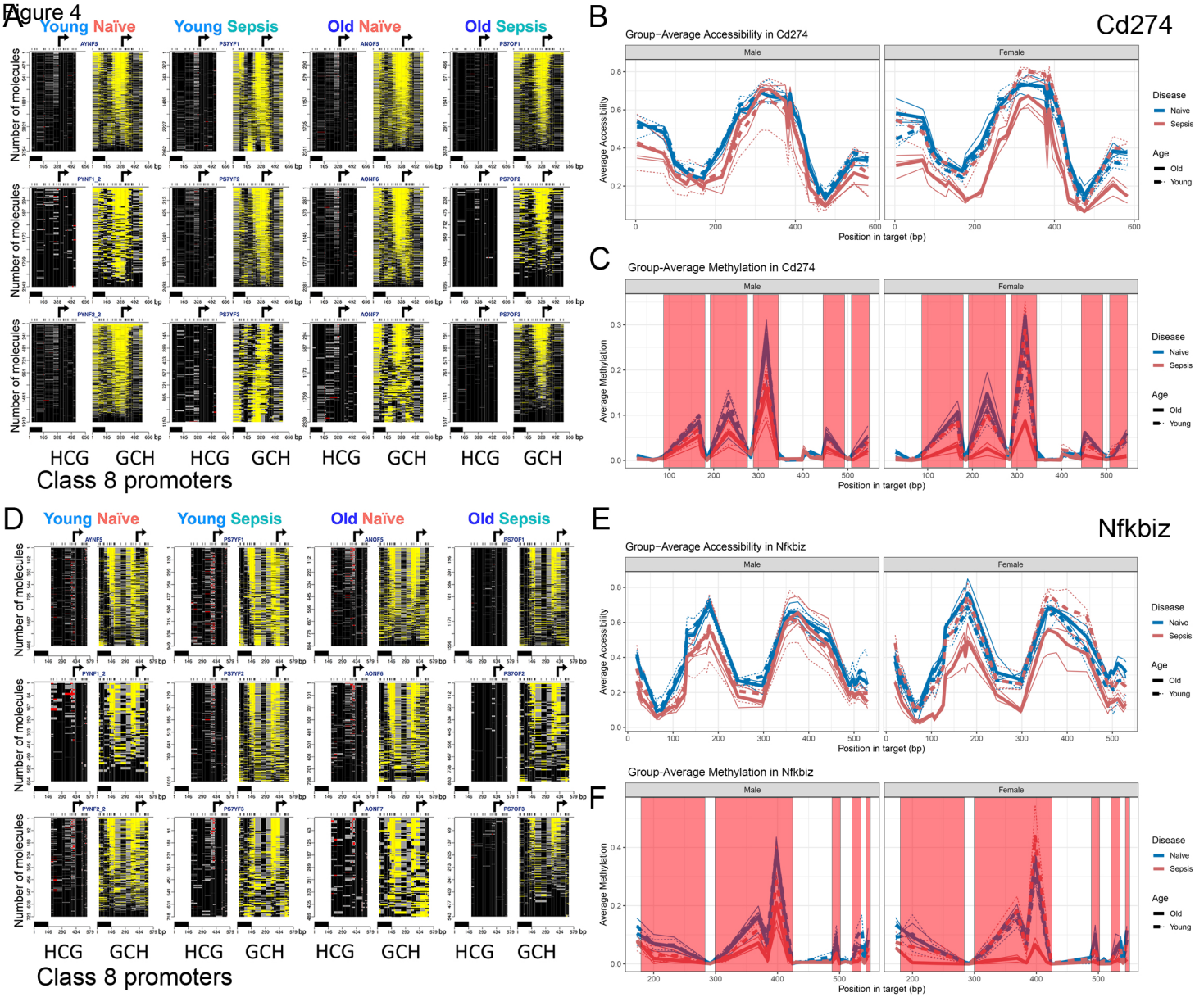
A
Young Naïve
Young Sepsis
Old Naïve
Old Sepsis
Number of molecules
HCG
GCH
Class 8 promoters
B
Cd274
Group−Average Accessibility in Cd274
Male
Female
Average Accessibility
Position in target (bp)
Disease
Naive
Sepsis
Age
Old
Young
C
Group-Average Methylation in Cd274
Average Methylation
D
E
Nfkbiz
Group−Average Accessibility in Nfkbiz
F
Group-Average Methylation in Nfkbiz

Figure 5

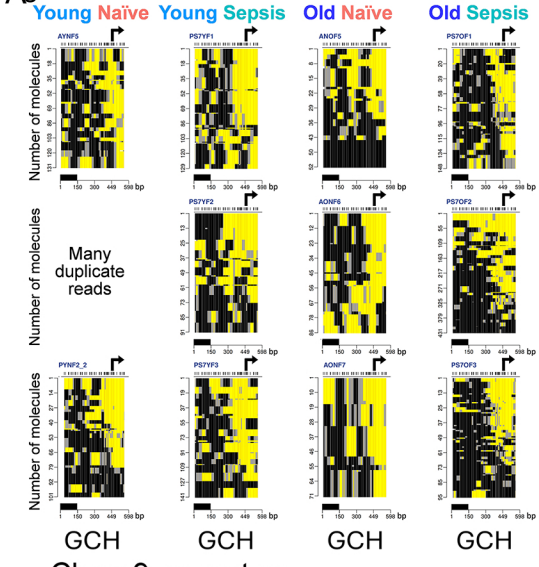
A
Young Naïve
Young Sepsis
Old Naïve
Old Sepsis
Number of molecules
Many duplicate reads
GCH
Class 9 promoters

B
Tet2
Group−Average Accessibility in Tet2
Male
Female
Average Accessibility
Position in target (bp)
Disease
Naive
Sepsis
Age
Old
Young

Figure 6

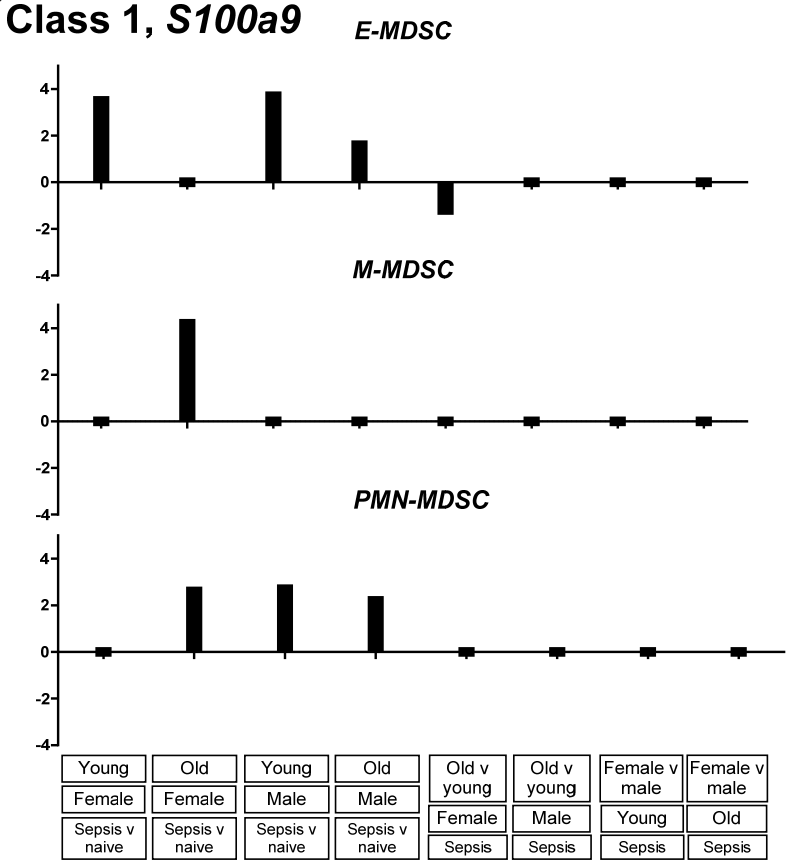
Class 1, S100a9
E-MDSC
M-MDSC
PMN-MDSC
4
2
0
-2
-4
Young
Female
Sepsis v naive
Old
Female
Sepsis v naive
Young
Male
Sepsis v naive
Old
Male
Sepsis v naive
Old v young
Female
Sepsis
Old v young
Male
Sepsis
Female v male
Young
Sepsis
Female v male
Old
Sepsis

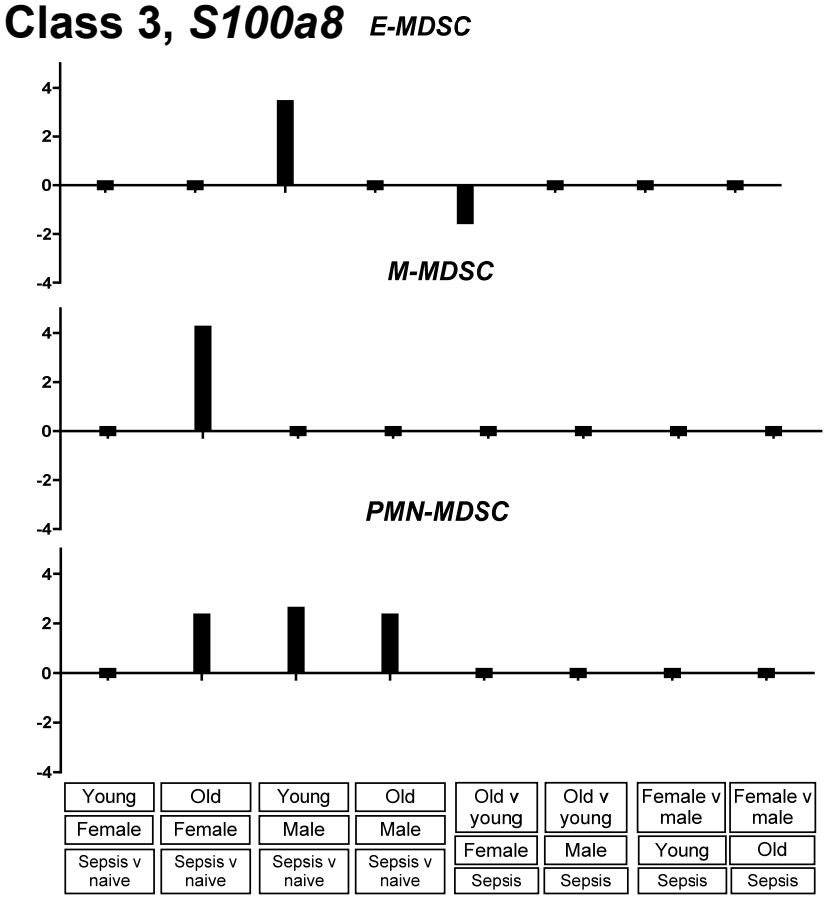
Class 3, S100a8
E-MDSC
M-MDSC
PMN-MDSC
4
2
0
-2
-4
Young
Female
Sepsis v naive
Old
Female
Sepsis v naive
Young
Male
Sepsis v naive
Old
Male
Sepsis v naive
Old v young
Female
Sepsis
Old v young
Male
Sepsis
Female v male
Young
Sepsis
Female v male
Old
Sepsis

Figure 7

Class 7, *Ccl5*

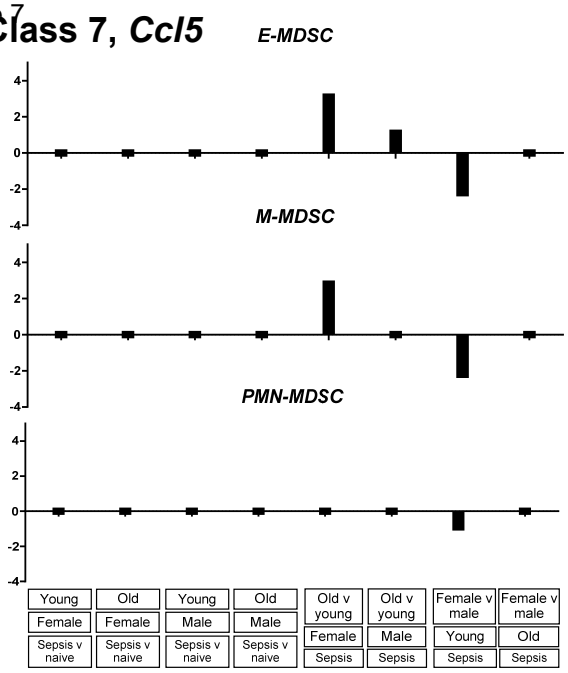

Class 8, *Nfkbiz*

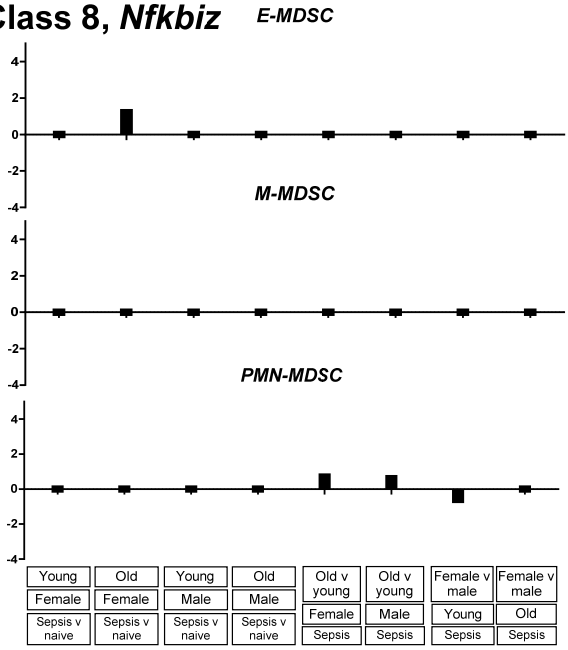

Class 9, *Tet2*

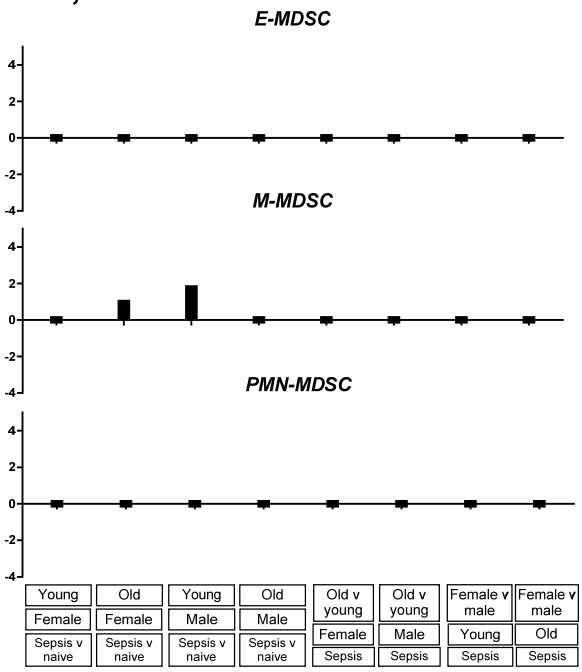

Click here to access/download;Supplemental Text and Figures;Charles_et_al_Supplemental.pdf

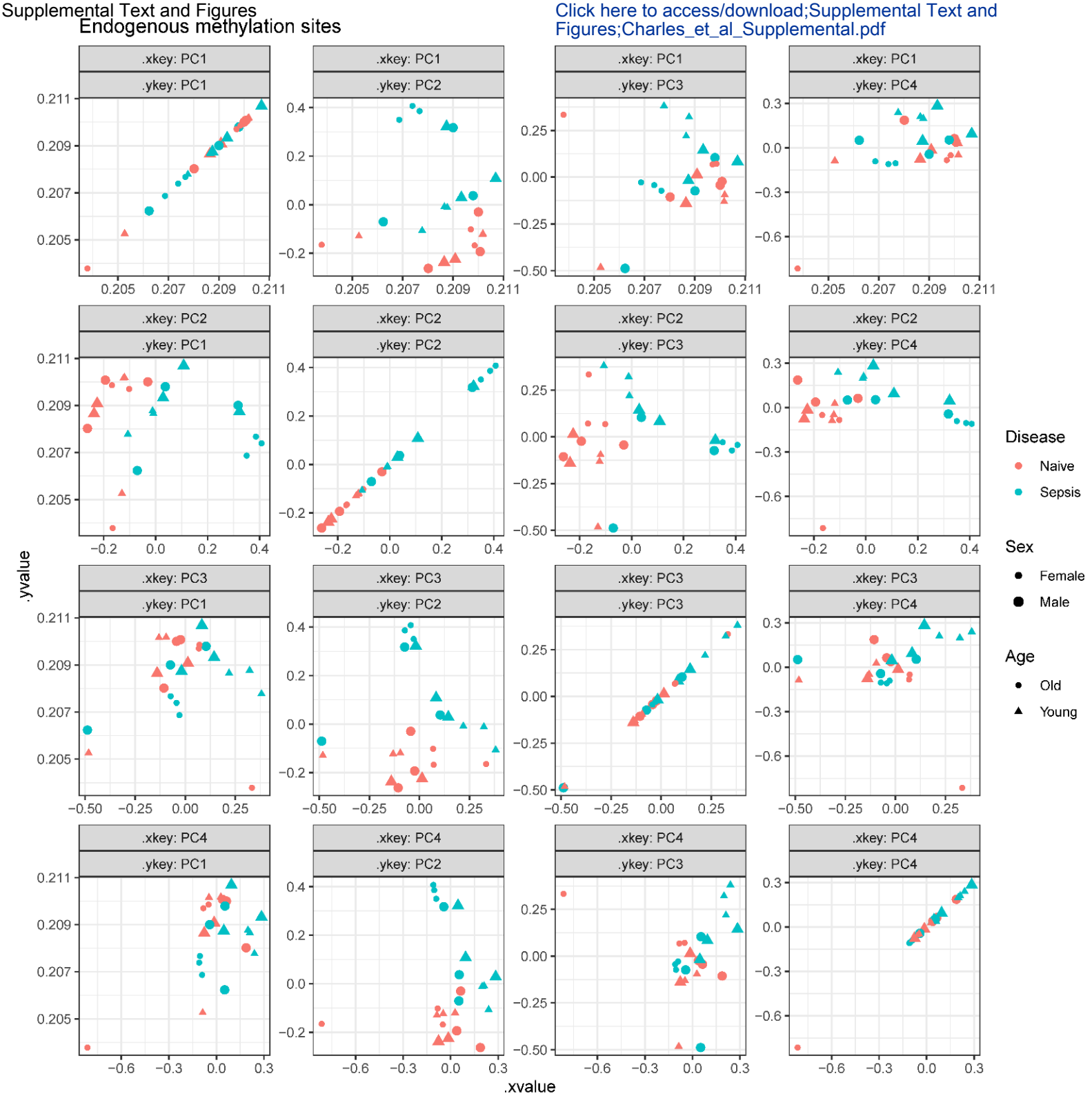

Supplemental Fig 1: **Principal component analysis (PCA) of endogenous CpG methylation (HCG) in splenic MDSCs.** PCA was performed on the percent methylation of CpG (HCG) sites across all covered promoters in CD11b^{+} Gr1^{+} MDSCs from male and female mice, young and old, with or without sepsis. Each point represents a single mouse. Color indicates disease condition (blue = naïve, red = sepsis), shape denotes sex (circle = female, triangle = male), and shading differentiates age (light = young, dark = old). Principal components 1-4 are plotted in pairwise combinations to visualize clustering. Old septic females exhibit distinct separation, indicating strong methylome remodeling in response to sepsis.

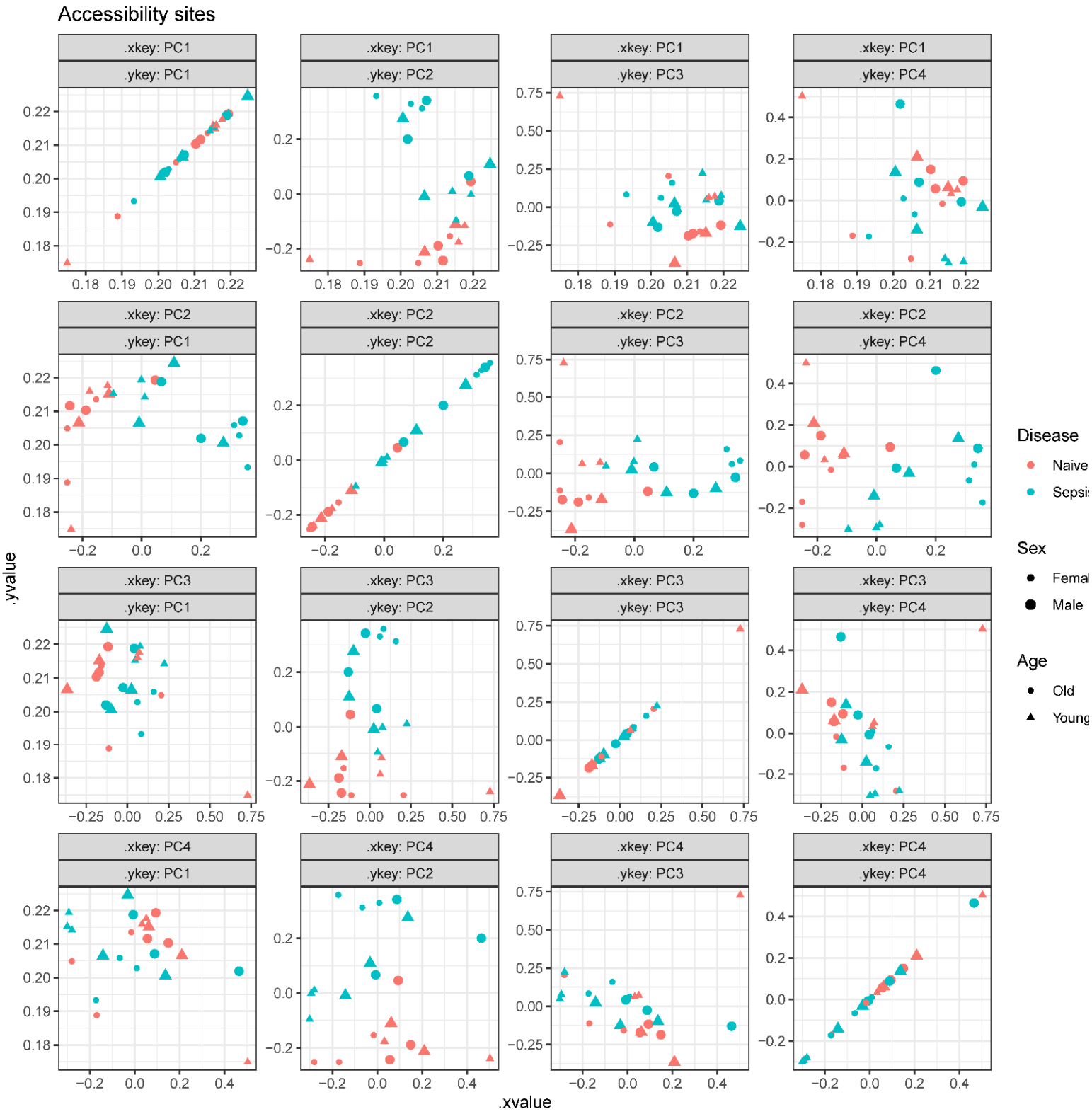

Supplemental Fig 2: **Principal component analysis (PCA) of GpC methylation (chromatin accessibility) in splenic MDSCs.** PCA was performed using GCH methylation values from MAPit-FENGC to reflect promoter accessibility across MDSC samples. Each point represents a single mouse. Color indicates disease condition (blue = naïve, red = sepsis), shape denotes sex (circle = female, triangle = male), and shading differentiates age (light = young, dark = old). Separation by sepsis status is evident across multiple PCs, with the strongest divergence observed in female mice. These results suggest widespread chromatin remodeling following sepsis, particularly in females.

Supplemental Table 1

Gene and Primer List used for MAPit-FENGC

Adgre1:ENSMUST00000086763
Akt1:ENSMUST00000001780
Ambp:ENSMUST00000030041
Arg1:ENSMUST00000020161
Atf6:ENSMUST00000027974
C3ar1:ENSMUST00000042081
Car4:ENSMUST00000103194
Car6:ENSMUST00000030817
Ccl12:ENSMUST00000000194
Ccl17:ENSMUST00000034232
Ccl2:ENSMUST00000000193
Ccl3:ENSMUST00000001008
Ccl5:ENSMUST00000035938
Ccl7:ENSMUST00000021011
Ccr1:ENSMUST00000026911
Cd247:ENSMUST00000161971
Cd274:ENSMUST00000016640
Cd63:ENSMUST00000219317
Cd74:ENSMUST00000167610
Cd9:ENSMUST00000032492
Cebpb:ENSMUST00000070642
Ctsl:ENSMUST00000222517
Cxcl2:ENSMUST00000200681
Cxcl3:ENSMUST00000031326
Cxcr2:ENSMUST00000106899
Cybb:ENSMUST00000015484
Dab2:ENSMUST00000159552
Dcn:ENSMUST00000105287
Dnmt3b:ENSMUST00000072997
Egln3:ENSMUST00000039516
Emp1:ENSMUST00000205156
F7:ENSMUST00000033820
Fabp7:ENSMUST00000020024
Fam20c:ENSMUST00000026972
Fgr:ENSMUST00000030693
Fosb:ENSMUST00000003640
Fyb:ENSMUST00000090461

Gpnmb:ENSMUST00000204260
Gprc5b:ENSMUST00000008878
Hdac3:ENSMUST00000043498
Htr2a:ENSMUST00000036653
Ighm:ENSMUST00000177715
Igkv12-44:ENSMUST00000103367
Igkv12-46:ENSMUST00000103365
Igkv4-69:ENSMUST00000103349
Igkv8-24:ENSMUST00000103384
Igkv9-120:ENSMUST00000103316
Iglv1:ENSMUST00000103746
Il10:ENSMUST00000016673
Il1r2:ENSMUST00000027243
Il1rl2:ENSMUST00000194296
Il4ra:ENSMUST00000033004
Il6:ENSMUST00000026845
Irf8:ENSMUST00000160943
Jun:ENSMUST00000107094
Kdm6b:ENSMUST00000094077
Lcn2:ENSMUST00000050785
Lgals1:ENSMUST00000089377
Lgals2:ENSMUST00000044584
Lgals3:ENSMUST00000151405
Lgals9:ENSMUST00000108268
Lrp1:ENSMUST00000049149
Lyz1:ENSMUST00000092162
Mmp19:ENSMUST00000026411
Mmp8:ENSMUST00000018765
Mmp9:ENSMUST00000137626
Mt2:ENSMUST00000034214
Nfkbiz:ENSMUST00000036273
Nos2:ENSMUST00000018610
Nrf1:ENSMUST00000115212
Plac8:ENSMUST00000031264
Pmp22:ENSMUST00000108702
Ptgs2:ENSMUST00000035065
Retn:ENSMUST00000012849
Rnase2a:ENSMUST00000061936
Ros1:ENSMUST00000020045
S100a10:ENSMUST00000045756
S100a8:ENSMUST00000069927

S100a9:ENSMUST00000117167
Saa3:ENSMUST00000006956
Serpina1a:ENSMUST00000072876
Serpinb1a:ENSMUST00000076352
Serpine1:ENSMUST00000041388
Slc7a2:ENSMUST00000057784
Sparc:ENSMUST00000214685
Spp1:ENSMUST00000086833
Stab1:ENSMUST00000036618
Stat3:ENSMUST00000103114
Tet2:ENSMUST00000098603
Tgfb1:ENSMUST00000002678
Timp3:ENSMUST00000020234
Tmem176a:ENSMUST00000204482
Tmem176a:ENSMUST00000204482
Tnfaip3:ENSMUST00000019997
Vcan:ENSMUST00000109546
Vdr:ENSMUST00000023119
Vegfa:ENSMUST00000071648
Vnn1:ENSMUST00000041416
Vsig4:ENSMUST00000050707
Atp6v0d2:ENSMUST00000029900
Dnase1l3:ENSMUST00000026315
Gm5849:ENSMUST00000180151
Hdac9-1
Hdac9-2
Igkv1-117:ENSMUST00000103317
Igkv6-15:ENSMUST00000103393
Igkv8-28:ENSMUST00000197525
Trem1:ENSMUST00000048782
Map3k1:ENSMUST00000109267
Ikbkg:ENSMUST00000164101
Ash1l:ENSMUST00000186583
Btk:ENSMUST00000033617
Cd180:ENSMUST00000170878
Cxcl15:ENSMUST00000031322
Cxcr4:ENSMUST00000052172
Foxo1:ENSMUST00000053764
Gdf5:ENSMUST00000040162
Hsf1:ENSMUST00000226860
Hsf2bp:ENSMUST00000238192

Hsf4:ENSMUST00000173102
Hsf5:ENSMUST00000093956
Hsfy2:ENSMUST00000062085
Hsp90aa1:ENSMUST00000155242
Hsp90ab1:ENSMUST00000024739
Hspa1a:ENSMUST00000087328
Hspa1b:ENSMUST00000172753
Hspa2:ENSMUST00000080449
Ifna1:ENSMUST00000094972
Ifna2:ENSMUST00000105147
Ifng:ENSMUST00000068592
Ikbkb:ENSMUST00000033939
Il12a:ENSMUST00000029345
Il12b:ENSMUST00000102796
Il3ra:ENSMUST00000224163
Il6:ENSMUST00000026845
Irak1:ENSMUST00000114354
Irak4:ENSMUST00000109248
Irf3:ENSMUST00000003284
Irf5:ENSMUST00000167252
Irf7:ENSMUST00000106023
Lbp:ENSMUST00000146600
Ly86:ENSMUST00000021860
Mapk1:ENSMUST00000232611
Mapk13:ENSMUST00000233984
Mapk14:ENSMUST00000004990
Mapk15:ENSMUST00000160092
Mapk3:ENSMUST00000050201
Mapk4:ENSMUST00000091851
Mapk6:ENSMUST00000049355
Mapk8:ENSMUST00000111945
Mme:ENSMUST00000194134
Myd88:ENSMUST00000035092
Nfkb1:ENSMUST00000029812
Nfkb2:ENSMUST00000237330
Nfkbia:ENSMUST00000021413
Nfkbib:ENSMUST00000032815
Nr2c2:ENSMUST00000113460
Pik3ap1:ENSMUST00000059672
Pik3c2a:ENSMUST00000170430
Pik3c2g:ENSMUST00000218528

Pik3c3:ENSMUST00000115812
Pik3ca:ENSMUST00000108243
Pik3r1:ENSMUST00000055518
Pik3r2:ENSMUST00000034296
Pik3r3:ENSMUST00000030464
Pik3r5:ENSMUST00000021283
Pik3r6:ENSMUST00000102613
Ptpn6:ENSMUST00000171549
Rela:ENSMUST00000025867
Src:ENSMUST00000109533
Tab1:ENSMUST00000229320
Tab2:ENSMUST00000146444
Tlr2:ENSMUST00000029623
Tlr4:ENSMUST00000107365
Tnf:ENSMUST00000025263
Traf6:ENSMUST00000004949
Vav1:ENSMUST00000169220